3-14-2008

Analyzing Carbohydrate-Based Regenerative Fuel Cells as a Power Source for Unmanned Aerial Vehicles

Olek Wojnar

Analyzing Carbohydrate-Based Regenerative Fuel Cells as a Power Source for Unmanned Aerial Vehicles

THESIS

Olek Wojnar, Captain, USAF

AFIT/GAE/ENY/08-M31

DEPARTMENT OF THE AIR FORCE
AIR UNIVERSITY

AIR FORCE INSTITUTE OF TECHNOLOGY

Wright-Patterson Air Force Base, Ohio

AFIT/GAE/ENY/08-M31

Analyzing Carbohydrate-Based Regenerative Fuel Cells as a Power Source for Unmanned Aerial Vehicles

THESIS

Presented to the Faculty

Department of Aeronautics and Astronautics

Graduate School of Engineering and Management

Air Force Institute of Technology

Air University

Air Education and Training Command

In Partial Fulfillment of the Requirements for the

Degree of Master of Science in Aeronautical Engineering

Olek Wojnar, BS

Captain, USAF

March 2008

AFIT/GAE/ENY/08-M31

Analyzing Carbohydrate-Based Regenerative Fuel Cells as a Power Source for Unmanned Aerial Vehicles

Olek Wojnar, BS
Captain, USAF

Approved:

Maj Eric D. Swenson (Chairman)	14 Mar 08 Date
Lt Col Christopher M. Shearer (Member)	14 Mar 08 Date
Lt Col Frederick G. Harmon (Member)	14 Mar 08 Date

Abstract

Based on current capabilities, we examine the feasibility of creating a carbohydrate-based regenerative fuel cell (CRFC) as the primary power source for unmanned aerial vehicles (UAV) for long endurance missions where station keeping is required. A CRFC power system is based on a closed-loop construct where carbohydrates are generated from zooxanthellae, algae that create excess carbohydrates during photosynthesis. The carbohydrates are then fed to a carbohydrate fuel cell where electric power is generated for the UAV's propulsion, flight control, payload, and accessory systems. The waste products from the fuel cell are used by the zooxanthellae to create more carbohydrates, therefore mass is conserved in the process of power generation. The overall goal of this research is to determine if CRFCs should be explored further as a viable power source. Through simulations, a UAV is sized to determine if greater than 24 hour endurance flight is possible and these results are compared to UAVs using more traditional photo-cell based power systems. The initial results suggest that more research should be done in the development of CRFCs as a power system for long endurance UAVs. The final outcome of this research is to identify the most important areas for more detailed follow-on work in designing a production-ready CRFC power system for long endurance UAVs.

Acknowledgements

Thanks to Dr. Heil for suggesting that students talk to him if they have any unconventional thesis ideas, and for agreeing to take a risk on a very far-fetched thesis. I would also like to thank Dr. Heil for his efforts in facilitating contact with the Air Force Research Laboratory (AFRL) both to support my thesis and to allow me to continue similar work after graduation.

Maj Swenson, thank you for your eager acceptance of my thesis after Dr. Heil's retirement. I appreciate all the helpful mentoring. Despite the fact that my topic was outside your principal area of expertise, I noticed that you made a concerted effort to learn a good deal of new material in order to provide better feedback to me. That has not gone unnoticed or unappreciated.

I also appreciate the numerous people both at AFRL and at AFIT who took the time to give me feedback and suggestions. Your involvement has improved both the content and the documentation of my work. I am very grateful.

Finally, I would like to thank all the people who were there for me when I was stressed or discouraged in the winding course of this work. You know who you are and I want you to know how much your support means to me. Thanks!!

Olek Wojnar

Table of Contents

Page

List of Figures

List of Tables

List of Symbols

Symbol		Page
C_D	Coefficient of drag	18
D	Aerodynamic drag	18
P_{prop}	Propulsion power required	18
P_{total}	Total power required	18
μm	Micrometer	20
$\eta_{FuelCell}$	Fuel cell efficiency	20
$P/W_{FuelCell}$	Power to weight ratio of fuel cell	20
g	Acceleration due to gravity	21
W_E	Empty weight	21
ρ_{algae}	algal density	23
t_{algae}	algae layer thickness	23
$C_{glucose}$	mass concentration of glucose in water	23

List of Abbreviations

Abbreviation		Page
NIE	Near-infinite endurance	1
NASA	National Aeronautics and Space Administration	2
CRFC	Carbohydrate-based regenerative fuel cell	3
UAV	Unmanned aerial vehicle	5
PAR	Photosynthetically active radiation	5
PEM	Polymer electrolyte membrane	8
Li-I	Lithium Ion	8
HALE	High-altitude long-endurance	17

Analyzing Carbohydrate-Based Regenerative Fuel Cells as a Power Source for Unmanned Aerial Vehicles

I. Problem Statement

There has been increased interest in recent years in the development of a persistent aerial platform to perform surveillance and communications. Aircraft powered by expendable fuel sources are unsuitable for persistent applications due to their severe endurance limits, and satellites are unsuitable due to their high cost and inability to loiter over specified areas of interest. An optimum solution would be a synthesis of the two technologies. This has been referred to as "near space" and involves long-endurance aircraft flying near the edge of the atmosphere to provide both persistence and mission-specific station-keeping [*Air University Center for Strategy and Technology*, 2007].

High-altitude vehicles would be most useful if they had a near-infinite endurance (NIE). In other words, an endurance which is not directly limited by fuel capacity but instead by mission parameters such as useful mission length. The idea of extending endurance through novel fuel choices is not a new one. Previous work has investigated various options for long-endurance flight and met with both success and setbacks.

An aircraft with a consumable power source, such as a traditional gasoline-powered engine, will always be constrained by the amount of fuel that it can carry. With the possible exception of nuclear fuel, which is considered too dangerous for airborne use, the weight of fuel required for a mission spanning weeks, months, or beyond exceeds the weight capacity of existing aircraft. Airborne refueling was demonstrated in 1929 by the US Army Air Corps' flight of the Question Mark [*Rhodes*, 1993] as a means of allowing effectively unlimited endurance for an aircraft. However, airborne refueling is not without its own shortcomings. Tanker aircraft must regularly rendezvous with the subject aircraft in order to keep it supplied with fuel; this can be inefficient if the subject aircraft is loitering far from the refueling base or downright dangerous if the loiter location is deep within hostile territory. Even if neither of these is a factor, the

effort and expense of continual rendezvous make this an unattractive option, especially as we increase the number of subject aircraft which are simultaneously airborne.

An obvious solution is that a NIE vehicle carry a renewable fuel source and the capability to replenish it. The most common solution is for such a vehicle to carry batteries which are recharged by a system of photovoltaic cells. A limiting factor is the relatively low energy density of current batteries and therefore the battery weight required to achieve NIE. For example, the NASA Helios prototype (See Figure 1.1) flew with enough battery capacity for 5 hours of flight after sunset [*Curry*, 2007]. If Helios had carried enough batteries to fly until the next morning, the W_{TO} would have been increased by over 60% [*Buchmann*, 2006] which would make the aircraft too heavy to take off.

Figure 1.1: NASA Helios Prototype

Hydrogen has been suggested as an alternative energy storage medium. It has approximately 200 times the mass energy density of Lithium-Ion batteries and can be renewed using a regenerative fuel cell. A regenerative fuel cell works by consuming its fuel when power is required, in this case by combining hydrogen and oxygen into water,

and separating the product back into fuel and oxidizer when another power source is available. In the original plan for Helios, a series of solar cells would use electrolysis to generate hydrogen and oxygen from water during the daylight hours. The problem with hydrogen is that because it is such a light gas, it contains very little energy per unit volume. It must be significantly compressed to meet aircraft volume constraints and the weight of these high-pressure tanks and associated equipment effectively lowers hydrogen's impressive 143 MJ/kg gravimetric energy density to around 5.4 MJ/kg [*Freedom Car and Fuel Partnership*, 2005]. An ideal solution would be an aircraft powered by a gasoline regenerative fuel cell since this construct would combine very favorable energy density with a capability for renewable fuel. Unfortunately, the technology is not currently available to recreate gasoline from its combustion products in this manner. We must therefore consider other fuel sources for our regenerative fuel cell.

To make NIE systems achievable with current technology, we examine a novel energy production concept. Inspired by the efficient energy storage found in biological life forms, the feasibility of using glucose as the primary power source in a regenerative power system for aircraft is investigated. The earliest evidence of the potential of a glucose power source was the crossing of the English Channel by Dr. Paul MacCready's human-powered Gossamer Albatross in 1979 [*Curry*, 2008]. If glucose could provide sufficient power for this flight, then it seems reasonable that it would have even greater potential if systematically integrated into an aircraft design. We propose a power system in which glucose is generated by zooxanthellae, a type of photosynthetic algae[1], contained in a compartment called the photosynthetic skin and located below the transparent upper wing surface of the vehicle. This glucose is then consumed by a glucose fuel cell which generates power for the aircraft and whose waste products are used by the algae to produce additional glucose. This is a closed system and mass is conserved during these interactions. This concept will henceforth be referred to as a Carbohydrate-based regenerative fuel cell (CRFC). It is illustrated in Figure 1.2 and explained in greater detail in Section 3.1. Since glucose has approximately a 24 times higher energy density than current batteries [*Buchmann*, 2006] [*Food and Agriculture Organization of the United*

[1]The word "algae" is the plural form of "alga" while "algal" is the adjective form.

Nations, 2003], it seems reasonable to investigate such a system to determine its potential usefulness for the aforementioned applications.

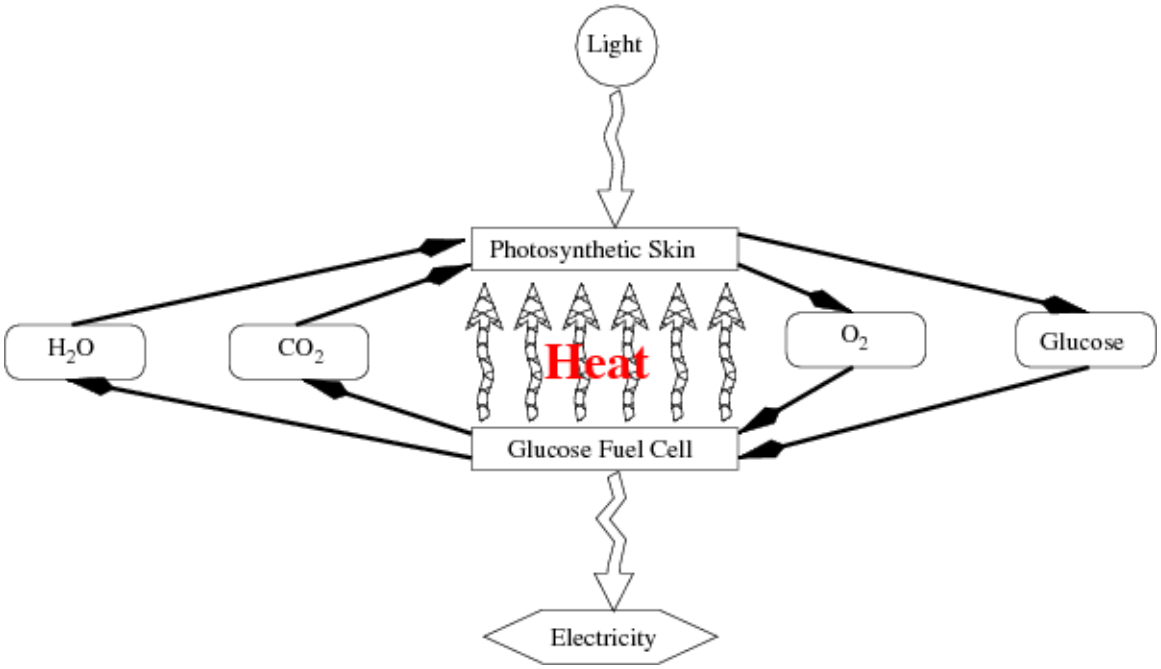

Figure 1.2: Carbohydrate-based regenerative fuel cell (CRFC)

The science required to create a functioning NIE platform is not trivial. The scientific background used in this work for CRFC power is explained in Chapter II and the method for synthesizing existing work into a functioning concept is detailed in Chapter III. Despite the extensive research performed for this work, there is undoubtedly additional useful material available. The results presented in Chapter IV represent an initial feasibility study and can be expanded given a sufficient investment of time and resources. This research aims to identify specific areas of the CRFC-powered NIE vehicle concept which would yield the greatest benefits with additional research. These target areas for improvement are identified in Chapter V.

II. Background

NUMEROUS areas of engineering must be combined in order to design an unmanned aerial vehicle (UAV) that is powered by a CRFC. These areas include the creation of usable glucose, conversion of glucose into electricity, and minimizing component weight. In the interests of clarity, the entire power system will be referred to as the CRFC while the portion of the system which converts glucose to electricity will simply be referred to as the glucose fuel cell.

2.1 Glucose Generation from Photosynthesis

On an industrial scale, glucose is normally produced from number 2 yellow dent corn [*Gray*, 1991]. One 25.4 kg bushel of corn will yield 15.1 kg of glucose [*Gray*, 1991]. However, this industrial process is not suitable for airborne application because it requires a corn input to create glucose. By contrast, the proposed system is closed and requires no external mass input to produce glucose. The proposed glucose production system is inspired by the symbiotic relationship between zooxanthellae algae and reef-building corals. The algae convert waste carbon dioxide (CO_2) and water (H_2O) into glucose ($C_6H_{12}O_6$) and oxygen (O_2) by the process of photosynthesis using incident sunlight as described by Equation (2.1) where h is Planck's constant, ν is the frequency of the light in Hertz (Hz) and the product $h\nu$ represents the light energy required for the reaction.

$$6CO_2 + 12H_2O + h\nu \rightarrow C_6H_{12}O_6 + 6O_2 + 6H_2O \tag{2.1}$$

There is a relationship between the intensity of incident light and the net production rate of glucose as shown in Figure 2.1 [*Fitt and Cook*, 2001]. The incoming energy is presented as a photon flux in units of micro Einsteins (μE) per square meter per second where micro Einsteins are micro moles of photons (μmol γ) of a given wavelength. A wavelength of 550 nm is normally used in calculations involving photosynthesis since this is the mean for the photosynthetically active radiation (PAR) wavelengths of 400 nm-700 nm [*Shulski et al.*, 2004]. This photon flux must be converted to units of $\frac{\mathrm{W}}{\mathrm{m}^2}$ (Watts per square meter) in order to calculate glucose production during various lighting condi-

tions. Equation (2.2) shows how this conversion is calculated where λ is the wavelength of the light in nanometers (nm) [*La Point et al.*, 1996].

$$\frac{\mathrm{W}}{\mathrm{m}^2} = \frac{\mu\mathrm{E}}{\mathrm{m}^2\,\mathrm{s}} \times \frac{119.6}{\lambda} \tag{2.2}$$

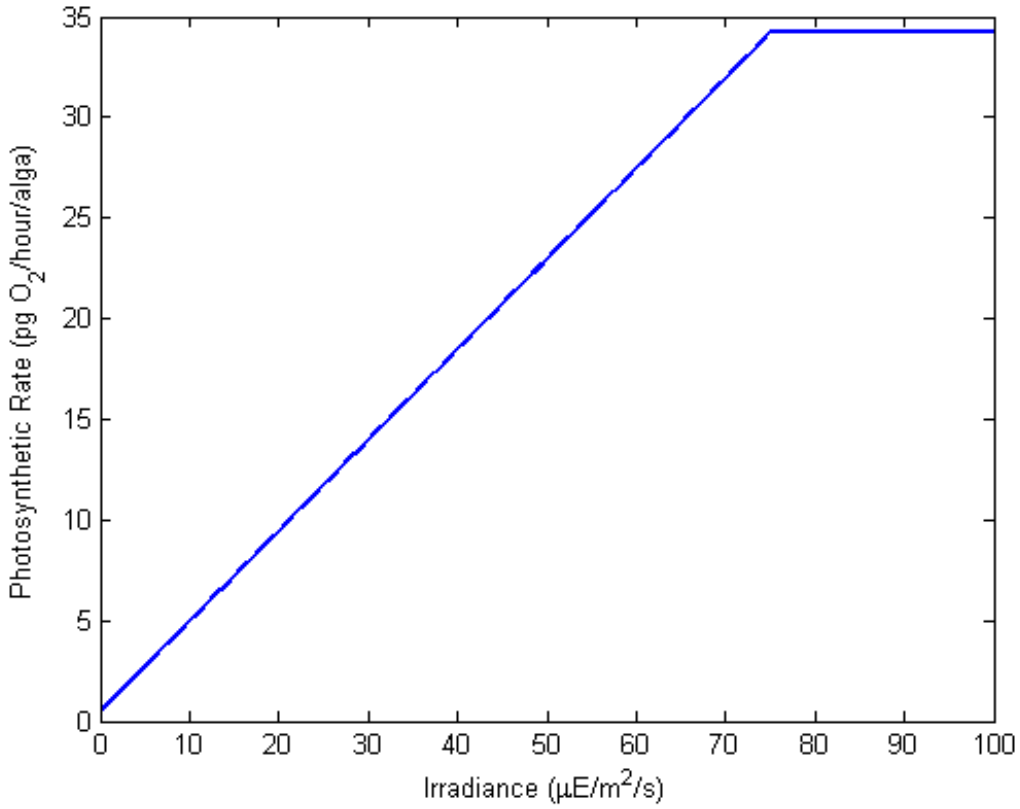

Figure 2.1: Laboratory Glucose Production Rate [*Fitt and Cook*, 2001].

The resulting photosynthetic rate is in units of picograms (pg) of oxygen per hour per zooxanthella, which can easily be converted to a glucose production rate as shown in Equations (2.3) and (2.4).

$$\frac{molO_2}{s \cdot alga} = \frac{pgO_2}{hour \cdot alga} \times \frac{gO_2}{1x10^{12}pgO_2} \times \frac{molO_2}{32gO_2} \times \frac{hour}{3600s} \tag{2.3}$$

$$\frac{kgC_6H_{12}O_6}{s \cdot alga} = \frac{molO_2}{s \cdot alga} \times \frac{molC_6H_{12}O_6}{6molO_2} \times \frac{180gC_6H_{12}O_6}{molC_6H_{12}O_6} \times \frac{kgC_6H_{12}O_6}{1000gC_6H_{12}O_6} \tag{2.4}$$

Photosynthetic rate is dependent on three parameters: PAR light intensity, temperature, and CO_2 concentration. Temperature would be regulated in this system and excess CO_2 provided so that the photosynthetic rate will continue to increase linearly with increasing PAR light intensity [*Garcia et al.*, 1994] as shown in the extrapolated dashed line in Figure 2.2. The solid line in Figure 2.2 represents the laboratory results of *Fitt and Cook* [2001] as previously shown in Figure 2.1. Combining the glucose production rate contained in Figure 2.2 and the unit conversions shown in Equations (2.2), (2.3), and (2.4), it is possible to determine how many kilograms of glucose will be generated given an irradiance in $\frac{\mathrm{W}}{\mathrm{m}^2}$.

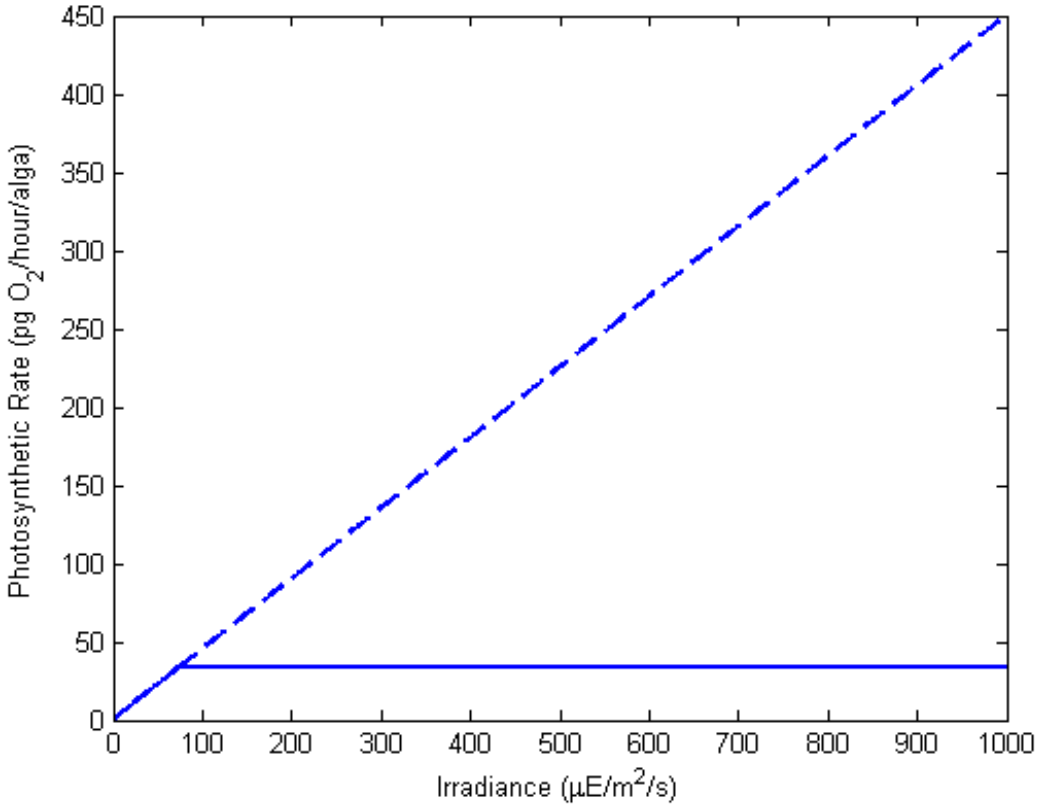

Figure 2.2: Extrapolated Glucose Production Rate [*Fitt and Cook*, 2001][*Garcia et al.*, 1994].

2.2 Converting Glucose into Electricity

One of the key enabling technologies for this project is the modern fuel cell. Recent research has yielded significant advances in fuel cell technology. On the simplest level, a

fuel cell is "a device that continuously changes the chemical energy of a fuel (as hydrogen) and an oxidant directly into electrical energy" [*Merriam-Webster Online*, 2007]. The key word in the definition is "directly." This directness is the major difference between fuel cells and most conventional means of generating electrical energy, such as turbines and internal combustion engines, in that the conventional methods normally have an intermediate step where the fuel is converted to mechanical energy, which results in a lower efficiency for indirect means of generating electricity. Fuel cells have yielded efficiencies as high as 81% [*Chaudhuri and Lovley*, 2003], making them suitable as an airborne power source where weight concerns make efficiency far more important than it is for most terrestrial applications. It is prudent to be very careful when comparing efficiencies reported by different researchers. As an example, one fuel cell was reported to have a 95% efficiency [*Weibel and Dodge*, 1975] however, upon closer inspection, it was revealed that this fuel cell only liberated 2 of the 24 electrons available in a glucose molecule and therefore had an overall efficiency of only 7.9%.

A generic polymer electrolyte membrane (PEM) fuel cell (See Figure 2.3) operates on hydrogen fuel with an oxygen oxidizer; a typical setup for most fuel cells. "(PEM) fuel cells-also called proton exchange membrane fuel cells-deliver high power density and offer the advantages of low weight and volume, compared to other fuel cells...(PEM) fuel cells operate at relatively low temperatures, around 80 °C" [*United States Department of Energy*, 2007]. In contrast, solid oxide fuel cells operate at temperatures up to 1000 °C [*United States Department of Energy*, 2007]. A variety of commercial uses exist for energy production from glucose, most commonly in the the wastewater treatment field [*Ehrenman*, 2004], however, the relatively higher energy density of conventional fuels such as gasoline (See Table 2.1) has limited the use of glucose as a fuel.

A regenerative fuel cell is essentially a highly advanced rechargeable battery system, and the fuel cell is the equivalent of just the discharge portion of the system. The fuel cell takes energy stored in the form of glucose or hydrogen and converts it to electricity as required. Table 2.1 clearly shows that even lithium ion (Li-I) batteries, which arguably have the best battery energy density by today's standards, fall far short of both hydrogen and glucose which can both be used to power a regenerative fuel cell. Note that the

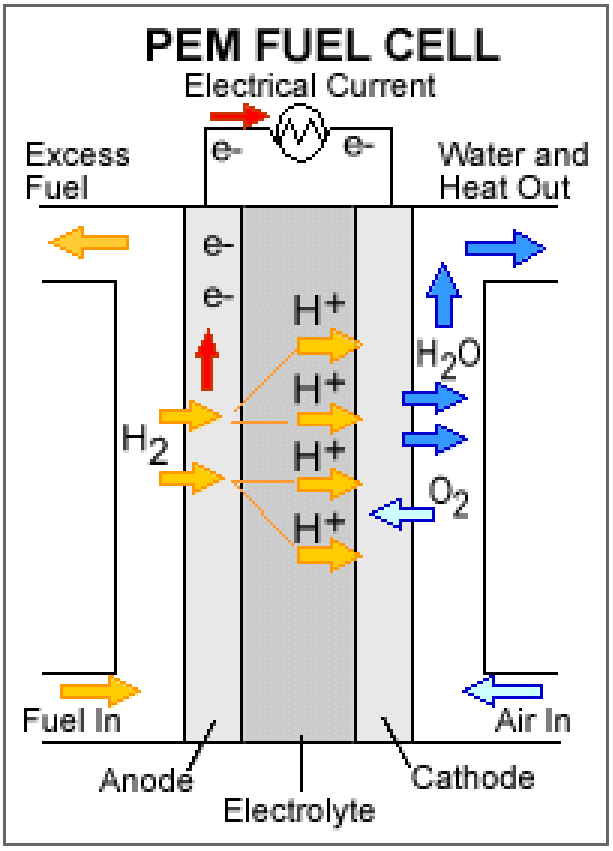

Figure 2.3: Generic Fuel Cell Schematic [*United States Department of Energy*, 2007].

information presented in Table 2.1 does not include the weight of fuel storage equipment or a means of converting the energy to usable power. The Li-I battery is the only fuel that will not suffer a penalty once storage and conversion weights are factored in. Since mass and volume are both critical design constraints for an aircraft, they must be minimized wherever possible. For the same amount of energy storage, using a Li-I battery requires

Table 2.1: Energy Density Comparisons [*Buchmann*, 2006] [*United States Department of Energy*, 2007] [*Turns*, 2000] [*Food and Agriculture Organization of the United Nations*, 2003]

Energy Source	Gravimetric Energy Density		Volumetric Energy Density	
	(MJ/kg)	(kWhr/kg)	(MJ/L)	(kWhr/L)
Li-I Battery	0.54 - 0.68	0.15 - 0.19	0.90 - 1.1	0.25 - 0.31
Compressed Hydrogen (10000 psi)	141.9	39.42	4.257	1.183
Gasoline (n-Octane)	44.8	12.4	31.5	8.75
Glucose	16	4.4	26	7.2

both more mass and more volume than hydrogen or glucose and therefore Li-I batteries, while simpler in design, are a suboptimal solution for the energy storage needs of an aircraft.

As fuel cell technologies develop, numerous new fuel sources are being investigated to overcome the shortcomings of hydrogen fuel [*United States Department of Energy*, 2007]. The usefulness of a glucose-based power source for medical implants has been one of the major drivers for the refinement of glucose fuel cells to date because the implant can be powered by the human body and does not require invasive surgery for periodic battery replacement [*Von Stetten et al.*, 2006]. Glucose is also an attractive alternative compared to hydrogen for future aircraft use because although hydrogen has a significantly higher gravimetric energy density, it has a much lower volumetric energy density. (See Table 2.1) This difference requires over five and a half times more volume to store an equivalent quantity of hydrogen fuel versus using glucose. Compressed hydrogen weighs over 8.4 times less than glucose for the same amount of energy, but these calculations do not take into account the significantly heavier fuel tank required to contain hydrogen at pressures around 10,000 psi, as well as equipment to reduce the pressure of the hydrogen as it is consumed and equipment to repressurize the regenerated hydrogen. Even using the most optimistic estimates, the net energy density of the hydrogen system will only be 5.4 MJ/kg [*Freedom Car and Fuel Partnership*, 2005]. This additional weight clearly offsets the benefits of using hydrogen. In addition to the energy density factors, glucose is a much safer fuel. As explained above, hydrogen must be compressed to very high pressures to achieve a reasonable volumetric energy density. This high pressure results in an inherent danger of a catastrophic tank rupture. While the chances of such a rupture can be minimized with robust tank construction, this serves to further reduce the gravimetric energy density of hydrogen. Even if a material was discovered for creating high-pressure storage tanks which were both light-weight and so strong as to virtually eliminate the danger of tank rupture, the hydrogen itself is flammable or explosive (depending on concentration) if released. In contrast, glucose can be stored at atmospheric pressure, is not explosive, and presents virtually no environmental impact in the event of a fuel spill.

As mentioned previously, direct glucose fuel cells are most applicable for medical applications [*Von Stetten et al.*, 2006], but their incomplete oxidation of glucose makes them inappropriate for a closed system such as a CRFC which requires the glucose to be fully broken down into carbon dioxide and water for subsequent photosynthetic glucose production. Microbial fuel cells use microbes such as *Rhodoferax ferrireducens* bacteria to completely break down glucose into carbon dioxide and water while providing self-regenerating characteristics absent in catalytic fuel cells [*Chaudhuri and Lovley*, 2003]. Microbial fuel cells are therefore ideally suited for the extraction of electrical energy from glucose in a CRFC. Three additional benefits of the Chaudhuri fuel cell are use of an inexpensive graphite electrode, no requirement for an additional mediator, and stable long-term performance. Many fuel cells use expensive precious metal electrodes as a catalyst which increases both the cost and weight of the fuel cell. These electrodes have also been known to degrade over time since they participate in the reaction which liberates electrons. Mediators are often used when the substance which breaks down the glucose is not able to readily transfer the liberated electrons to the electrode. They add expense and complexity and are often the shortest-lived component in the fuel cell. The stable long-term performance of this particular fuel cell is of great interest in a NIE platform because the aircraft can now be sized for the required mission and we can minimize additional factor-of-safety power which would otherwise be needed in anticipation of a degradation in power production over the life of the system. In contrast, a Li-I battery's capacity can fall to as little as 80% of its initial value in as little as 300 charge-discharge cycles, in addition the battery will lose some charge capacity from aging in as little as a year even without excessive cycling [*Buchmann*, 2006]. To counteract the capacity decrease over time, a greater mass of batteries would need to be carried on a UAV to continue providing a minimum power reserve.

2.3 Minimizing Weight

Since the glucose fuel cells mentioned in Section 2.2 are designed for terrestrial applications, they do not generate nearly enough power per unit mass. A relatively simple method of increasing this ratio is to use electrode materials with a higher surface

area to mass ratio. Recent studies on improved capacitors show that a surface area to mass ratio of 100,000 $\frac{m^2}{kg}$ is possible [*Zhang et al.*, 2001]. But the pores in this material, as well as all other porous nanomaterials described in recent literature, are far too small to accommodate the bacteria required to break down the glucose fuel [*Finneran et al.*, 2003]. This effectively reduces the surface area to that of a nearly flat sheet. Therefore, a sheet of nanotubes appears to be a simpler approach. Nanotube sheet electrodes can be created in a relatively high-volume method [*Zhang et al.*, 2005] which is very useful due to the large surface area that an airborne CRFC requires. These electrodes have a surface area to mass ratio of only 37,000 $\frac{m^2}{kg}$ [*Zhang et al.*, 2005] which will allow enough reaction surface area to generate the required power levels for the UAV without an excessive weight penalty.

III. Method

Synthesizing the research discussed in Chapter II, it is possible to create an aircraft powered by a CRFC as shown in Figure 1.2. Glucose is generated as discussed in Section 2.1, electricity is generated from this glucose as discussed in Section 2.2, and weight is minimized to allow flight as discussed in Section 2.3. The ultimate goal is to create a vehicle that can stay aloft almost indefinitely while performing a given mission. Such a mission might be to perform surveillance or act as a communications relay or anything else which would benefit from the NIE characteristics of this aircraft. In this work, a surveillance mission similar to that of the U.S. Air Force Global Hawk UAV is assumed. In order for this vehicle to have a NIE, for any given 24-hour period it must be able to extract enough energy from ambient light to fly and perform its mission for that entire time period. Since the vehicle will not have 24 hours of daylight, this means that it must be able to store enough exergy (the total amount of energy that can theoretically be converted to useful work, differentiated from useful energy by the efficiency of converting energy to work) to function during the time when exergy consumption is greater than exergy collection. For example, if we assume that the aircraft begins operations at a given time, it must produce enough excess exergy during the daylight hours to sustain operations at night and until the same time the next day. In addition, the exergy reserve at the same time the next day must be greater than or equal to what it was initially. If the vehicle can meet these two constraints, then it will have a NIE. An example of such an exergy over time analysis is shown in Figure 3.1.

Since a CRFC-powered NIE aircraft is a rather novel concept, the design is broken down into discrete sub-systems. This breakdown serves both to make the system easier to understand and also to simplify future improvements by creating a well-defined framework identifying the functions of each component and the interactions of all of the functions.

3.1 System Design

A systems engineering approach was used to break the CRFC UAV into functional components. This approach allows a more meaningful sorting of results in our analysis.

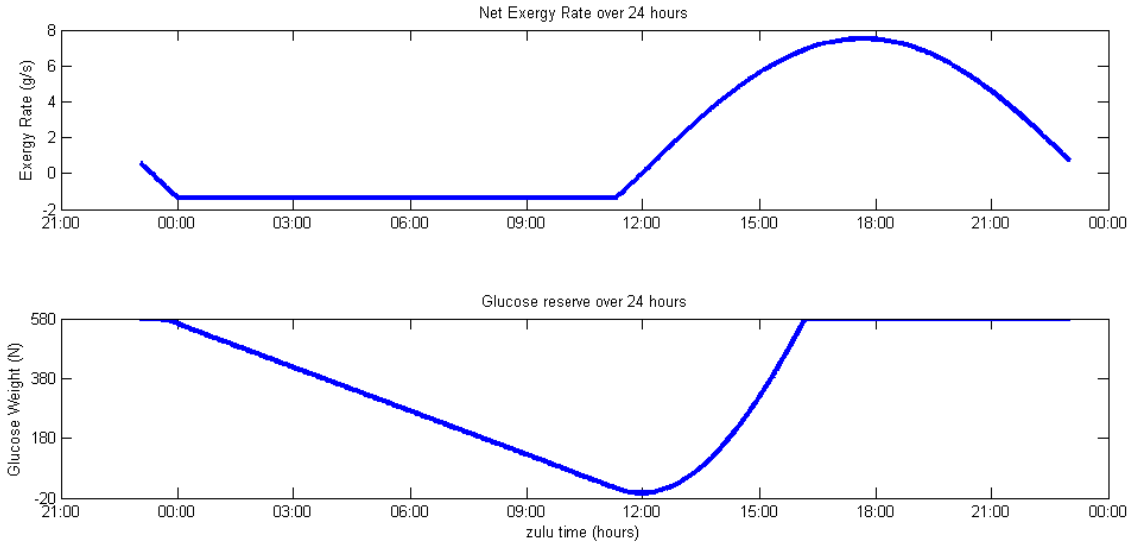

Figure 3.1: CRFC UAV flight timeline

Instead of making general suggestions, we can target specific components for further work. Figure 3.2 lists the components that make up the CRFC UAV power system. Note that these components satisfy the functions shown in the CRFC concept flowchart in Figure 1.2. The skin cover is added to separate the light attenuation and heat transfer reduction from the actual photosynthetic functions of the photosynthetic skin.

Figure 3.3 explains how the overarching requirement to provide power to the CRFC UAV is broken down and handled at the component level. We see that the power requirement is broken down into three sub-requirements: Generate Electricity, Generate Glucose and Transport Elements. The electricity generation requirement is accomplished by the Convert Glucose to Electricity function which is contained in the Glucose Fuel Cell component. The glucose generation requirement is composed of two functions:

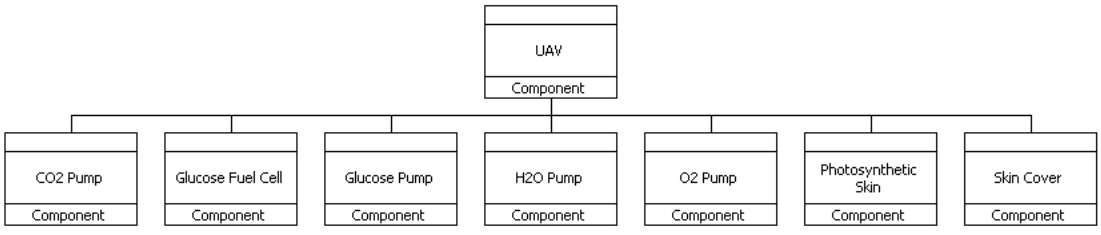

Figure 3.2: CRFC UAV power system components

Capture Light and Convert Light to Glucose. The Capture Light function is performed by the Skin Cover component while the Convert Light to Glucose function is performed by the algae-containing Photosynthetic Skin of the aircraft. Finally the requirement to transport elements is performed by the following four functions: Transport CO_2, Transport Glucose, Transport H_2O and Transport O_2. Each of these four functions is then performed by its respective pump.

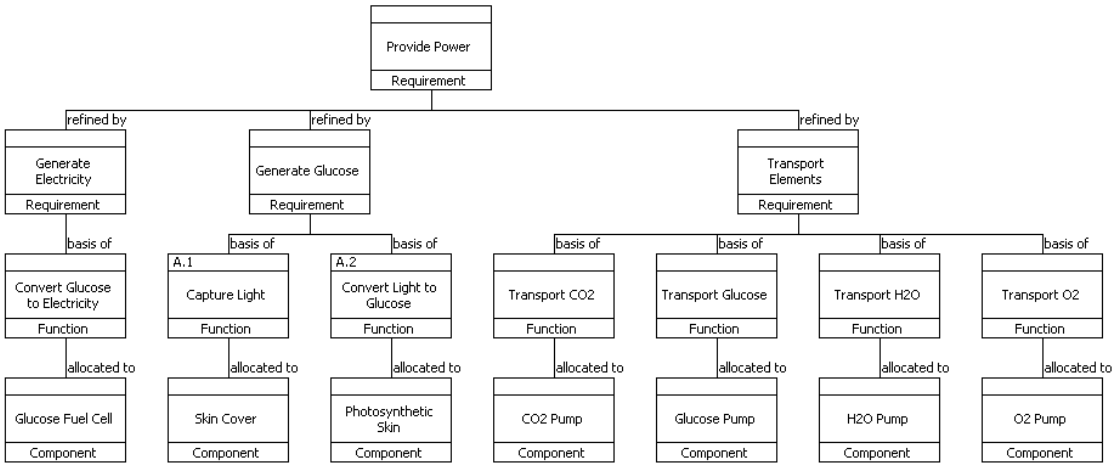

Figure 3.3: Provide Power Requirement.

Figure 3.4 details the interactions of the functions we have just described. Whenever light is incident on the vehicle, it performs the Capture Light and Convert Light to Glucose functions. This is slightly idealized since once the glucose reserves are full we will no longer be generating more glucose. All of the other components are controlled by the requirement to provide power. The four transports shuttle compounds between the Photosynthetic Skin and the Glucose Fuel Cell while the Glucose Fuel Cell converts the glucose it receives into electrical energy. Since semi-permeable membranes and methods for transporting liquids and gases are readily available, those aspects of the design will not be examined more closely in this work. These components would be significant if a working CRFC was created at some point in the future (See Section 5.1).

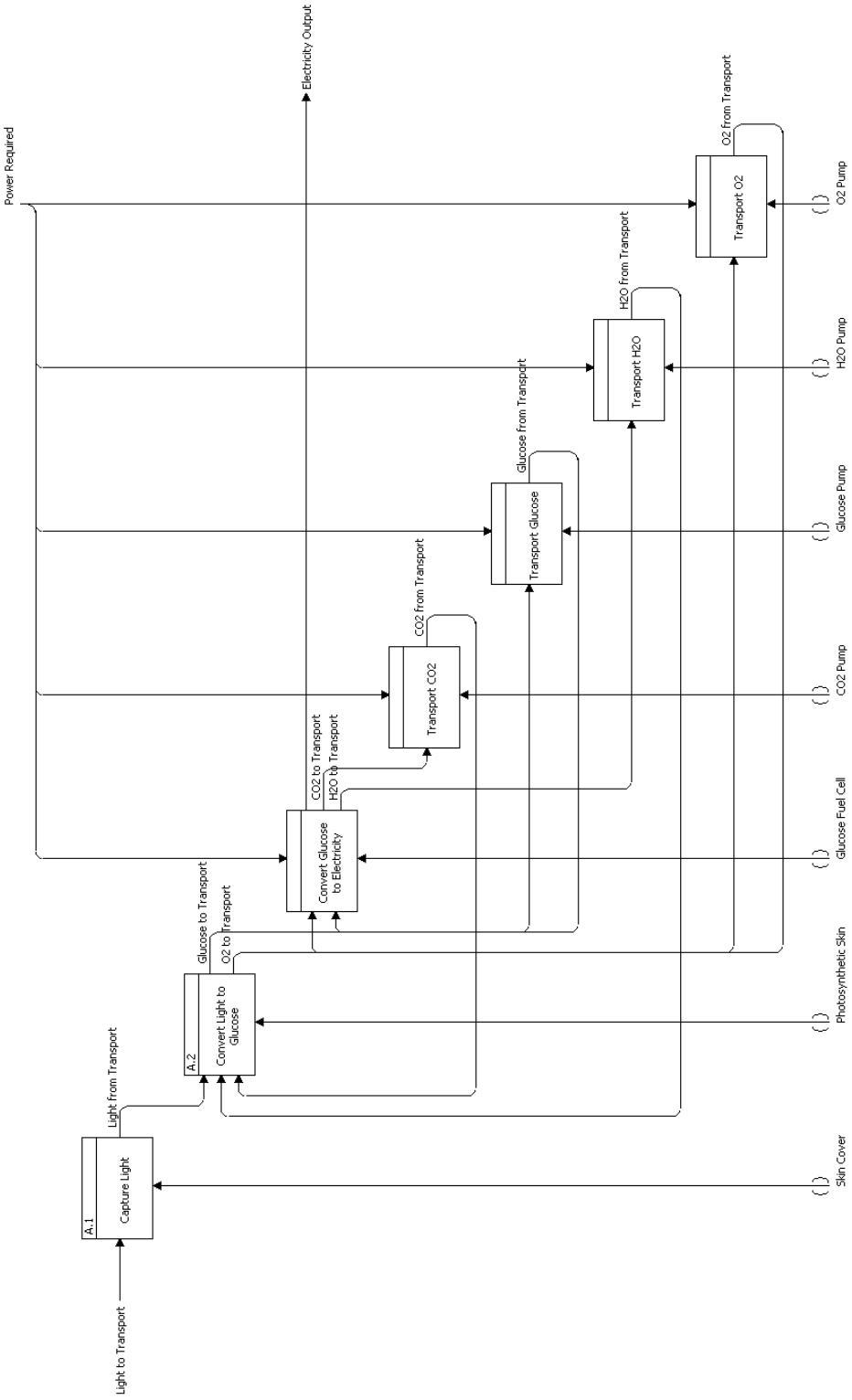

Figure 3.4: Provide Power Function.

3.2 Mission Parameters

A number of mission parameters are specified for this CRFC UAV study. As stated earlier, the Global Hawk UAV electro-optical and infrared sensor is used as the mission payload. This sensor has a mass ($m_{payload}$) of 136 kg and draws 600 W of power ($P_{payload}$) [*Hicks*, 2002]. The mass and power requirements of the payload are the most significant independent variables for sizing the aircraft because they have the greatest effect on the size of the powerplant, and therefore the aircraft, required to utilize them. Section 4.9 shows how much lighter a CRFC UAV with a similar configuration would be without payload mass and power requirements. A cruising altitude of 20 km is specified because this is very close to the maximum altitude of the Global Hawk UAV [*Hicks*, 2002] and therefore allows reasonable use of that UAV's sensor payload. This altitude is also used by *Harmats and Weihs* [1999] for their high-altitude long-endurance (HALE) vehicle and allows reasonable use of their vehicle parameters. Finally, this altitude is within the cruising altitude range of the Helios prototype and allows accurate comparisons with that aircraft. Wind and lighting conditions are different depending on location and time of year and while many different possibilities exist, (See Section 5.1) Dayton, OH on the 28th of March is chosen for this study. Average winds for this longitude, latitude, altitude, and time of year are between 15 m/s and 20 m/s [*National Oceanic and Atmospheric Administration*, 2008] therefore a cruise velocity (V) of 20 m/s is selected. It is possible that for missions where precise station-keeping is required this velocity will not be sufficient to counteract intermittent, higher-velocity winds. This would need to be examined more carefully for specific missions (See Section 5.1) and could be remedied by providing a reserve power capacity in the fuel cell to temporarily increase velocity over nominal cruise velocity. The PAR flux (E_{PAR}) is computed in two steps: first the maximum PAR (light with λ between 400 nm and 700 nm) is computed [*Dereniak and Crowe*, 1984] based on no atmospheric loss factors due to the high altitude. Next the PAR at a given date and time is computed based on the current angle of the sun [*Reda and Andreas*, 2004]. A propeller efficiency (η_{prop}) of 0.92 and an electric motor efficiency (η_{motor}) of 0.90 is used based on *Harmats and Weihs* [1999]. The algae layer covering is taken to be a lightweight, thermally insulating

plastic seal with a transmittance ($\eta_{SkinCover}$) of 0.99. The Oswald efficiency factor (e) is 0.9 because the CRFC UAV has a long and tapered wing. An auxiliary aircraft power (P_{aux}) of 20 W is assumed to power the flight control systems. The coefficient of lift (C_L) is computed using Equation (3.1) and is a function of the aircraft gross takeoff weight (W_{TO}), wing planform area (S), air density (ρ), and V. A value of 1.6 is considered the highest realistic value of C_L and configurations which result in higher numbers are discarded as infeasible.

$$C_L = \frac{2\,W_{TO}}{S\,\rho\,V^2} \tag{3.1}$$

The coefficient of parasitic drag (C_{D_o}) is 0.03 because of the streamlined shape of the vehicle. The coefficient of induced drag (C_{D_i}) is computed using Equation (3.2) and is a function of C_L, e, and aspect ratio (AR). The total coefficient of drag (C_D) is the sum of C_{D_o} and C_{D_i}.

$$C_{D_i} = \frac{C_L^2}{\pi\,e\,AR} \tag{3.2}$$

The drag (D) on the vehicle is then calculated using Equation (3.3).

$$D = \frac{1}{2}\,\rho\,V^2\,S\,C_D \tag{3.3}$$

The propulsion power required (P_{prop}) is calculated using Equation (3.4). P_{prop} is the primary component of total power required (P_{total}).

$$P_{prop} = D \times V \tag{3.4}$$

The P_{total} is the key factor in sizing the aircraft power system. It is computed using Equation (3.5).

$$P_{total} = \frac{P_{prop}}{\eta_{prop}\eta_{motor}} + P_{payload} + P_{aux} \tag{3.5}$$

This analytic approach and the equations used are commonly accepted and are found in most aircraft design textbooks.

3.3 Glucose Production

The glucose production subsystem is inspired by the symbiotic relationship between zooxanthellae algae and reef-building corals as explained in Section 2.1. The glucose used to power the aircraft is generated by zooxanthellae contained in a thin fluid-filled compartment below the transparent insulating upper surface of the UAV. This compartment is what we refer to as the photosynthetic skin. The algae convert waste carbon dioxide and water into glucose by the process of photosynthesis using incident sunlight. The two design variables in this component are the density of algae in the fluid and the thickness of the fluid layer. The algae layer is assumed to cover the entire upper surface area of the wing. Considering algae density, the greater the density the more glucose can theoretically be produced. However, once the algae concentration reaches a certain point, the algae lower in the layer will have their light supply blocked by the algae higher up in the layer and the photosynthetic output per alga is expected to decrease. This decrease needs to be modeled more accurately, preferably through laboratory measurements (see discussion on future work in Section 5.1). In this work, the skin is very thin and therefore light is assumed to fully reach all algae in the layer. In a terrestrial application where weight is not a concern and the skin thickness could be increased significantly, this assumption would break down and the aforementioned model would be very important in order to optimize the terrestrial photosynthetic skin design. Since the photosynthetic skin layer is conservatively assumed to weigh as much as the water it contains, because the weight of the algae is insignificant by comparison, we would like to get as much glucose production out of each unit mass of skin as possible. Considering the skin thickness, the greater the skin thickness the greater the percentage of incident light that is converted to glucose. With an infinitely thick skin, we could safely assume all the incident light would be available to be converted into glucose. However, the water content makes this skin very heavy and therefore we must try to minimize the weight while still producing as much glucose as possible (See Section 4.5).

3.4 Electrical Power Generation

The electrical power generation subsystem is a more mature technology than the glucose generation subsystem, based on published research into glucose fuel cells. However, the author is not aware of a previous attempt to apply this technology to an airborne platform and this presents an entirely new series of challenges. The most significant new challenge is that of weight. Specifically, the fuel cell must be able to generate enough power per unit weight to allow for powering the aircraft while not increasing the weight to the point that the aircraft is no longer capable of flight. In order to reduce the weight of the fuel cell, an electrode composed of carbon nanotubes as described in Section 2.3 is used instead of the graphite electrodes used by *Chaudhuri and Lovley* [2003] and described in Section 2.2. Since the *Rhodoferax ferrireducens* bacteria used in the fuel cell are approximately 3-5 μm long and 1 μm wide [*Finneran et al.*, 2003], the best electrode for this purpose is one which has an average pore size slightly larger than the size of this bacteria. However, since current nanoporous materials have pores on the order of 200 nm and smaller [*Zhang et al.*, 2001], a different solution must be investigated. The flat nanotube sheet electrode does not present pore size concerns and provides a good reaction surface area with a minimal weight penalty.

Chaudhuri and Lovley [2003] found that their fuel cell efficiency ($\eta_{FuelCell}$) is 0.81 and we assume that this does not change with the weight-reducing changes required for the CRFC. The power to weight ratio of our modified *Chaudhuri and Lovley* [2003] fuel cell ($P/W_{FuelCell}$) was computed according to Equation (3.6). $PowerDensity_{FuelCell}$ is 0.31 W/m^2 according to *Chaudhuri and Lovley* [2003], $AreaDensity_{FuelCell_{Electrode}}$ is 0.000027 kg/m^2 according to *Zhang et al.* [2005], and $AreaDensity_{FuelCell_{Electrolyte}}$ is assumed to be 0.00104 kg/m^2. The value of $AreaDensity_{FuelCell_{Electrolyte}}$ is based on an electrolyte layer that is slightly thicker than the 1 μm width of the *Rhodoferax ferrireducens* bacteria. This is a reasonable assumption because *Chaudhuri and Lovley* [2003] note that almost all of the power production from their fuel cell was the result of bacteria attached to the electrode and not the bacteria floating in solution. Therefore, the extra

fluid in the fuel cell merely wastes weight and is removed for this application. It should be noted that the value g in Equation (3.6) is the acceleration due to gravity.

$$P/W_{FuelCell} = \frac{PowerDensity_{FuelCell}}{(AreaDensity_{FuelCell_{Electrode}} + AreaDensity_{FuelCell_{Electrolyte}}) \times g} \quad (3.6)$$

$P/W_{FuelCell}$ is thus determined to be 2.94 W/N.

3.5 Aircraft Design Factors

Aircraft structural weight is normally estimated from previous similar aircraft in the initial design process. Since the Helios prototype is generally accepted to be the current pinnacle of HALE flight, its empty weight (W_E) is a reasonable estimate of the CRFC UAV's W_E. To produce more meaningful comparisons, our calculations are based on a W_E that does not include the weight of the power system. An official W_E for the Helios prototype is not publicly available. We start with the takeoff mass of Helios (599.64 kg [*Curry*, 2007]), subtract an estimated mass of Helios' solar cells and batteries and we obtain a reasonable estimate of W_E for Helios. The value of Helios' S (183.58 m^2 [*Curry*, 2007]) is multiplied by an estimate of weight per unit area of photovoltaic cells (0.45 kg/m^2 [*Harmats and Weihs*, 1999]) to obtain the mass of Helios' solar cells (82 kg). Since nearly the entire wing surface of Helios is covered with photovoltaic cells [*Curry*, 2007], this is a reasonable estimate. For the battery weight, it is known from *Curry* [2007] that Helios could fly for approximately 5 hours after sunset. Since Helios consumed 10 kW of power in level flight [*Velev*, 2000] and the gravimetric energy density of Li-I batteries is approximately 190 Wh/kg [*Buchmann*, 2006], the battery mass is approximately 263 kg. This yields an empty mass of 254 kg and a W_E of 2490 N. This value of W_E was multiplied by a scaling factor of CRFC UAV wingspan divided by the Helios wingspan of 75.29 m [*Curry*, 2007] to obtain an empty weight for various wingspans as shown in Equation (3.7). The CRFC UAV W_{TO} was computed by taking

the sum of W_E, payload weight, computed fuel cell weight, computed glucose reserve weight, and computed algae layer weight.

$$W_E = \frac{2490}{75.29} \times wingspan \tag{3.7}$$

IV. Results and Discussion

VARIOUS ranges of aircraft specifications are examined in order to show how certain design and technology choices affect the final size of the aircraft. Throughout this chapter the following vehicle parameters are used unless otherwise specified:

- $V = 20$ m/s - Cruise velocity
- $\rho_{algae} = 5.5681 \times 10^{14}$ algae/m^3 - Density of algae in photosynthetic skin
- $t_{algae} = 0.0001$ m - Thickness of algae layer
- $P/W_{FuelCell} = 2.94$ W/N - Power to weight ratio of fuel cell
- $C_{glucose} = 0.45 \ \frac{\text{kg}_{\text{glucose}}}{\text{kg}_{\text{glucose+water mixture}}}$ - Concentration by weight of glucose in water
- $wingspan = 100$ m - Aircraft wingspan
- $AR = 30.9$ - Aircraft aspect ratio

In each of the following sections, a sensitivity analysis on select variables is performed to determine the best avenues for future research. The results are constrained by realistic values of C_L, (See Section 3.2) and the requirement to achieve NIE (See Chapter III introduction). If either constraint is not met the data point is rejected and will not be shown below. Once we examine the factors that influence the CRFC UAV design, we will compare key specifications of this proposed CRFC UAV with specifications for NASA's Helios prototype.

4.1 Cruising Velocity

Both takeoff weight and required power are sensitive to the choice of cruising velocity. This dependence is a parabolic relationship so the further the design value is from the optimum value the more rapidly the efficiency of the design deteriorates. Figure 4.1 shows that 14 m/s is the lowest power cruising velocity. 4 m/s below to 6 m/s above that value also yield a similar power requirement but greater deviations result in a suboptimal or unfeasible design. Too low a value will require an impossible C_L to maintain flight and too high a value will require too much power and will not allow NIE. Equation 4.1 shows how the required propulsion power was calculated for various cruising velocities.

Note that D is a function of altitude, airspeed, and geometry of the wing as shown in Equation (3.3).

$$P_{prop} = D \times V \tag{4.1}$$

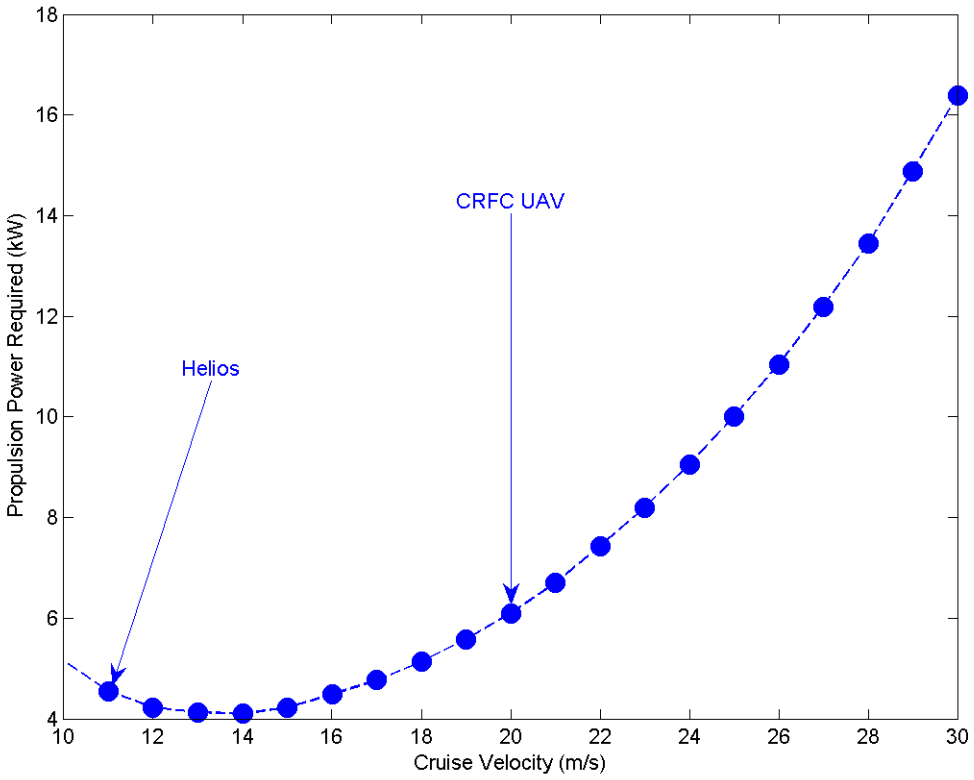

Figure 4.1: Relationship between propulsion power required and cruise velocity

Figure 4.2 shows that 20 m/s allows for a relatively low vehicle weight while still maintaining station-keeping. This assumes that winds speeds [*National Oceanic and Atmospheric Administration*, 2008] do not excess the average often or for long durations. Since 20 m/s is also near the maximum efficiency from Figure 4.1, it is the most reasonable value to use. Equation (4.2) shows the factors which contribute to the gross takeoff weight. Note that the weight of the fuel cell is proportional to the power required from it (Equation (4.1)) and since we are assuming a fuel cell which has not been optimized for flight conditions (See recommendations in Section 5.1), increases in required power significantly increase the weight of the fuel cell. In addition, a larger fuel cell also requires

a larger glucose reserve weight to supply the fuel cell and possibly a higher algae layer weight to replenish the glucose reserve.

$$W_{TO} = W_E + W_{payload} + W_{FuelCell} + W_{GlucoseReserve} + W_{AlgaeLayer} \tag{4.2}$$

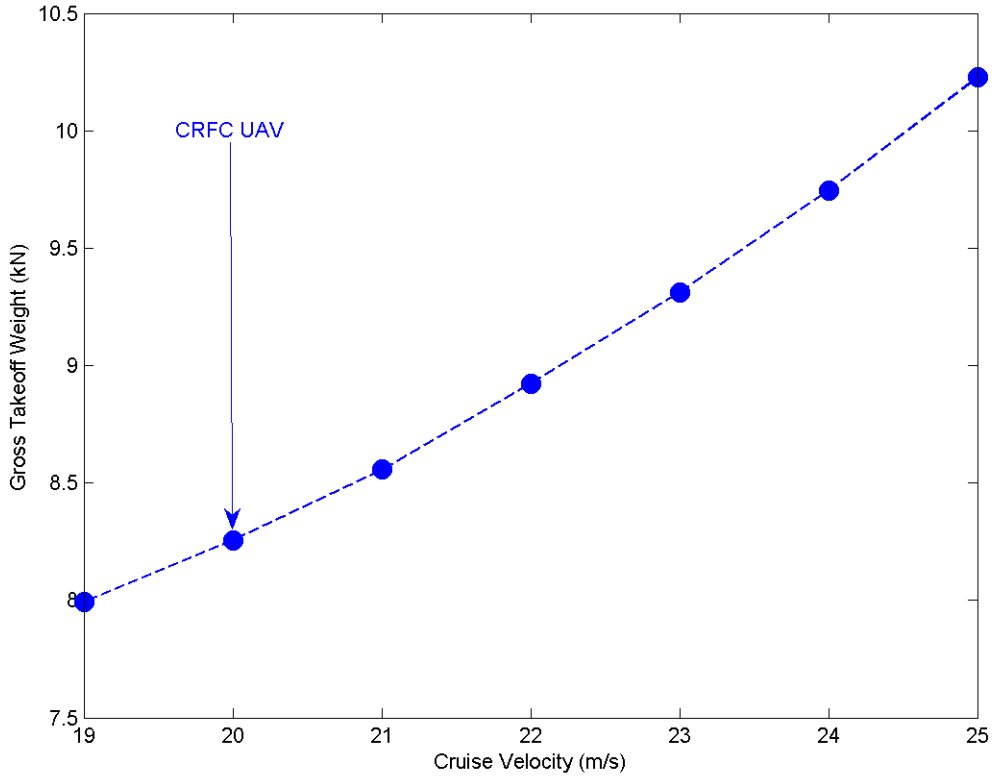

Figure 4.2: Relationship between gross takeoff weight and cruise velocity

4.2 Concentration of Glucose Solution in Storage Tanks

Chaudhuri and Lovley [2003] used a low glucose concentration (0.001) in their fuel cell. Storing the entire glucose supply at this concentration would result in carrying a massive weight in excess water. If the glucose is stored at a higher concentration and diluted prior to consumption in the fuel cell, immense weight savings can be realized. Figure 4.3 shows that significant weight savings are possible by increasing the concentration of stored glucose. If the stored glucose concentration is too low, the aircraft will be too heavy to fly because of the extra water weight. This is shown in the lower con-

centration limit on the graph. Values much above our chosen value of 0.45 run the risk of glucose coming out of solution [*Bishop*, 2005] and possibly clogging up critical flow paths. Therefore a $C_{glucose}$ value of 0.45 is used from this point forward in our analysis.

$$C_{glucose} = \frac{m_{glucose}}{m_{glucose+water\ mixture}} \tag{4.3}$$

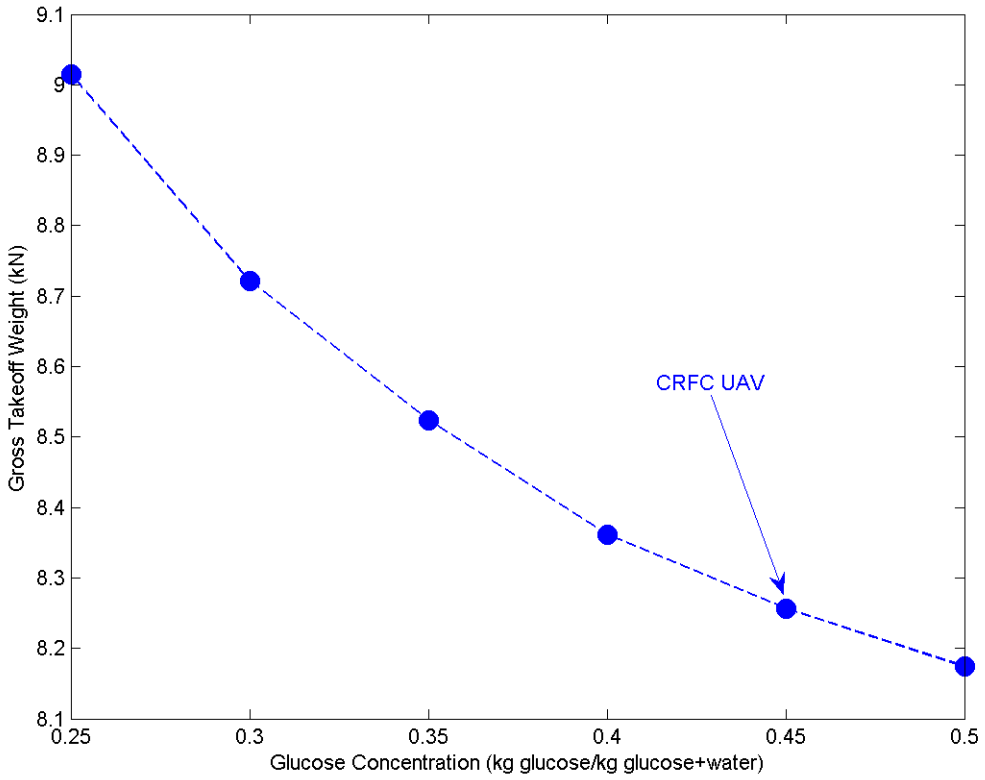

Figure 4.3: Relationship between gross takeoff weight and glucose solution concentration

4.3 Power to Weight Ratio of Glucose Fuel Cell

As seen in Figure 4.4, the power to weight ratio of the fuel cell has the greatest effect on W_{TO} between values of around 3 to values of around 10. In that range, the W_{TO} of the vehicle can be reduced by over 2000 N (over 26 %) from its peak value at $P/W_{FuelCell}$=2.94 W/N. The power to weight ratio is normally determined from Equation (4.4) (See Section 3.4) however, in this exercise, we attempt to estimate the $P/W_{FuelCell}$

to determine what values are required for a flight-weight glucose fuel cell so as to create a functional CRFC UAV.

$$P/W_{FuelCell} = \frac{PowerDensity_{FuelCell}}{(AreaDensity_{FuelCell_{Electrode}} + AreaDensity_{FuelCell_{Electrolyte}}) \times g} \quad (4.4)$$

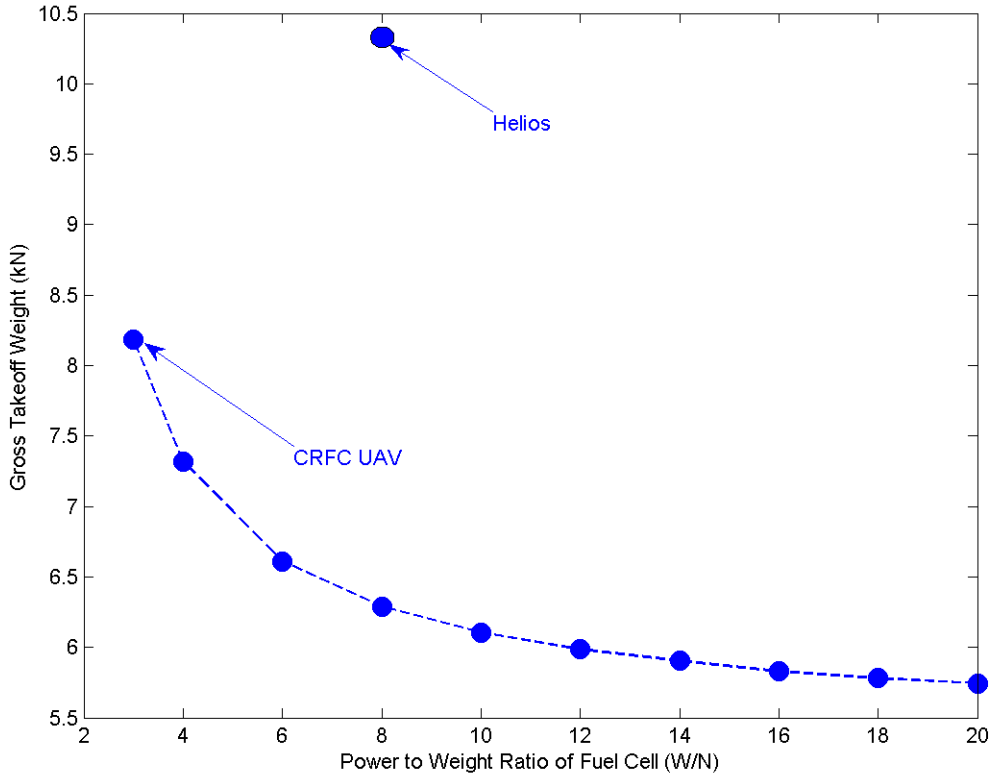

Figure 4.4: Relationship between gross takeoff weight and $P/W_{FuelCell}$

4.4 Algal Density in Photosynthetic Skin Layer

The density of algae in the photosynthetic layer is crucial for glucose production to achieve NIE. Higher density values allow for thinner photosynthetic layers and smaller wingspans, both of which decrease the aircraft weight and simplify the structural design. Figure 4.5 shows a several-fold increase in glucose production rate with increasing algal density. There is a finite limit to the number of zooxanthellae that can be packed into a

given space while still allowing transport of materials to and from the algae. However, an additional increase in photosynthetic rate can be achieved either by increasing the density of chloroplasts[1] in the zooxanthellae, and therefore their photosynthetic capability, or by finding another organism to generate glucose with a higher yield per unit volume.

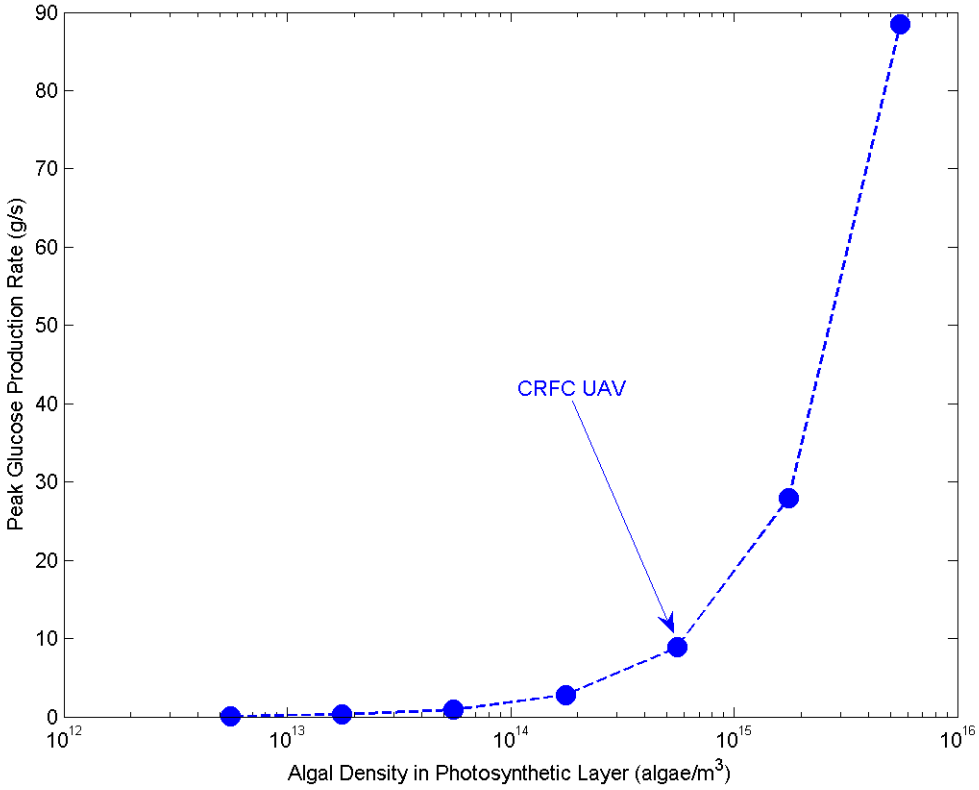

Figure 4.5: Relationship between peak glucose production rate and algal density

4.5 Thickness of Photosynthetic Skin Layer

Even very small changes in the thickness of the photosynthetic algae layer have a significant impact on the weight and overall feasibility of the design. Since the aircraft would have a wing planform area of a few hundred square meters, adding even a small amount of water depth across that entire surface results in enormous weight changes. In fact, this parameter is so sensitive that there is only a very narrow range of thicknesses which yield a usable design. This narrow range is shown in Figure 4.6.

[1] A chloroplast is the part of a non-bacterial cell responsible for the photosynthetic process.

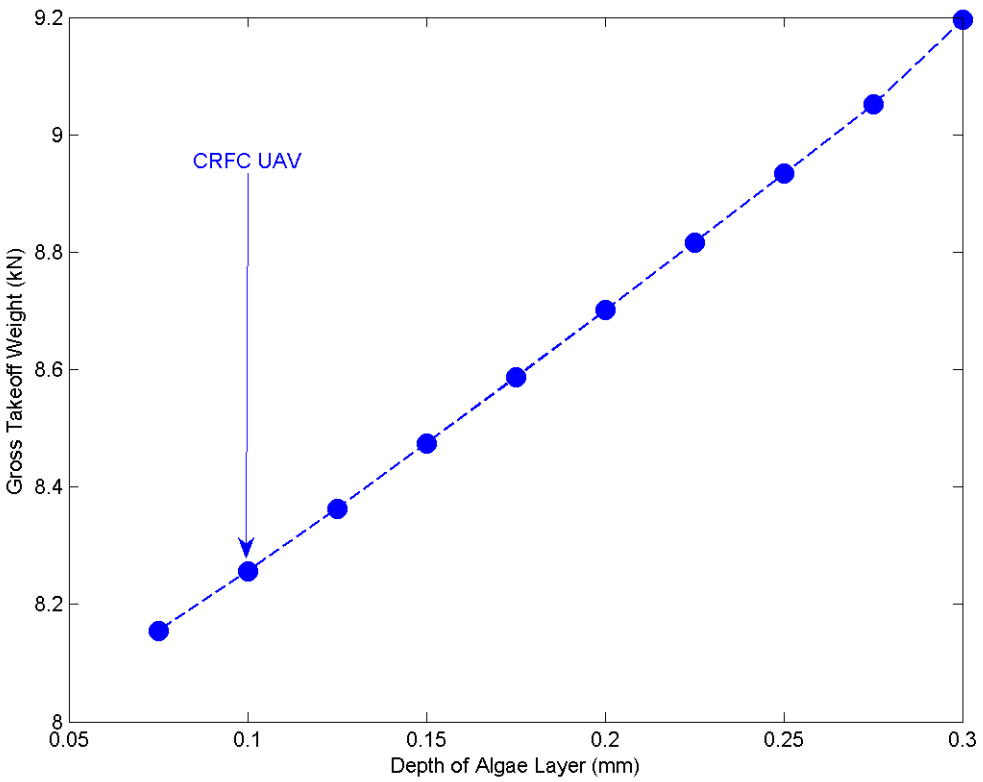

Figure 4.6: Relationship between gross takeoff weight and algae layer thickness

Values greater than the displayed range result in an aircraft which is too heavy to fly, while values which are too low do not allow enough algae for daytime glucose regeneration. The relationship between layer thickness and glucose production is shown in Figure 4.7. Note that this increases linearly since a thicker layer allows more algae to be present and produce glucose. Non-linear effects are not considered since the layer depth at which linear assumptions would no longer be reasonable is significantly greater than the depth at which the layer becomes too heavy for airborne applications. However, non-linear effects would be very significant for terrestrial applications as discussed in Section 5.1. Also note that the glucose production rate determines the speed at which our exergy reserve regenerates but it is unrelated to available power which is determined by the size of the fuel cell. If a method was found to increase the photosynthetic rate in the skin (See Section 4.4), the skin weight could be decreased beyond the lower limit shown in Figure 4.7.

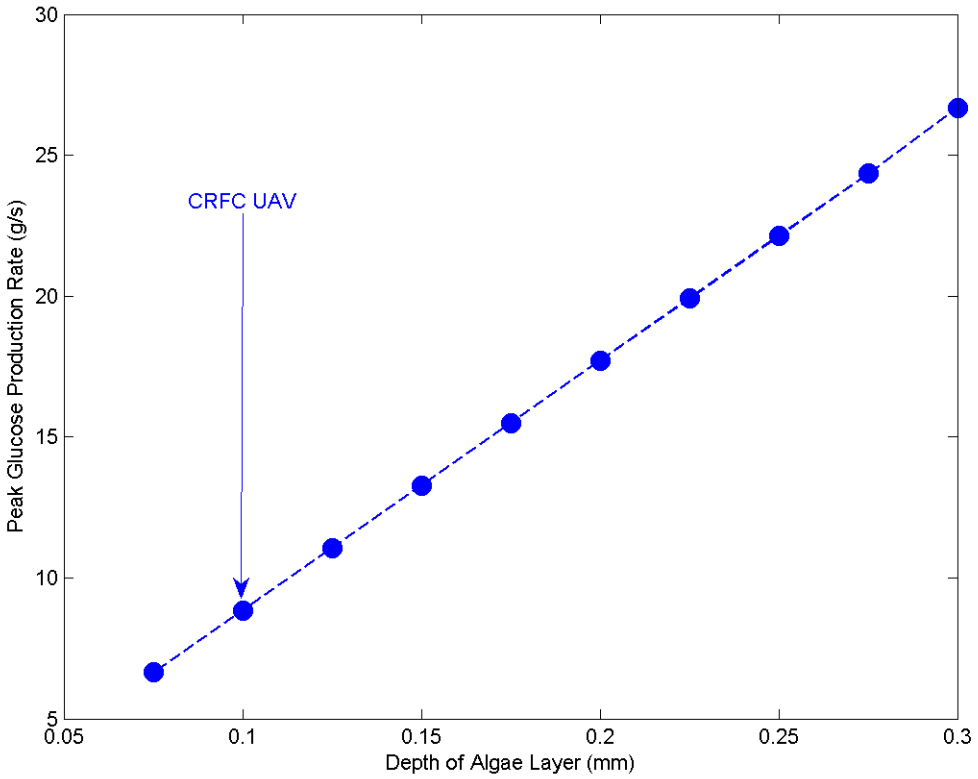

Figure 4.7: Relationship between peak glucose production rate and algae layer thickness

4.6 Saturation Light Intensity

Saturation light intensity is the light intensity at which additional light no longer increases the photosynthetic rate. This is because either temperature or CO_2 availability is limiting the photosynthetic reactions (See Figure 2.2). Since CO_2 from the fuel cell is being supplied directly to the algae, CO_2 availability is assumed to not limit the photosynthetic reactions, as is the case in Figure 2.1. Laboratory results show a significantly lower light intensity plateau [*Fitt and Cook*, 2001] which we believe is most likely caused by poor transport of CO_2 to the algae. The upper bound shown in Figure 4.8 represents the limiting condition of all available sunlight being utilized. If more incoming light was available it could also be utilized and the graph would extend further.

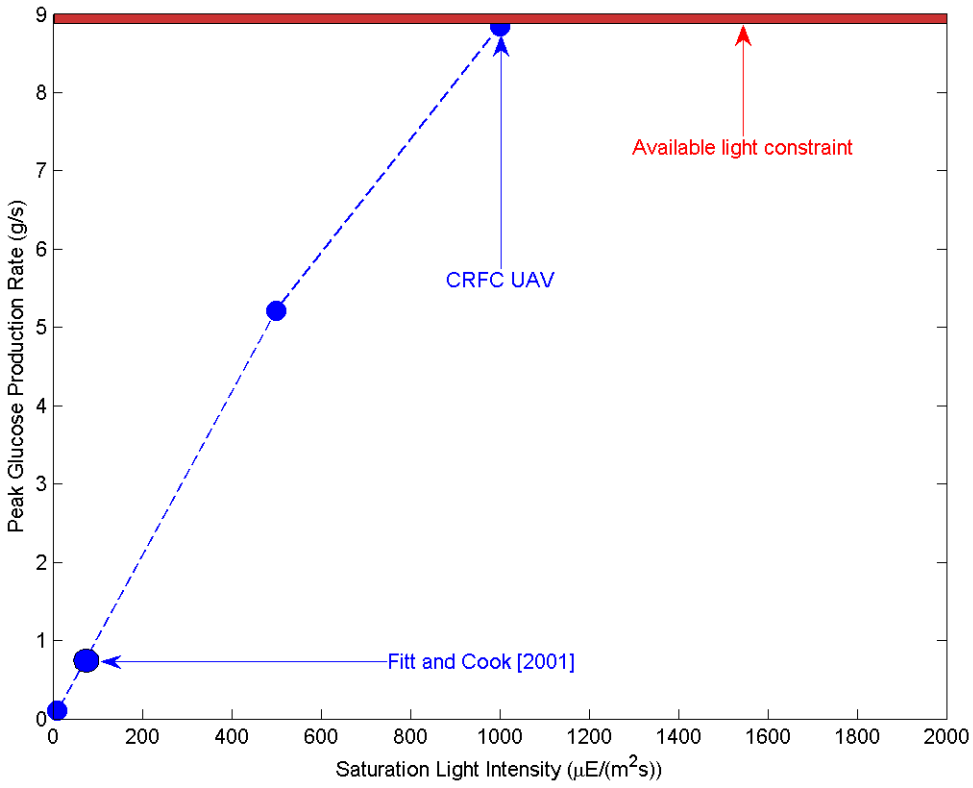

Figure 4.8: Relationship between peak glucose production rate and saturation light intensity

4.7 Aspect Ratio

Aspect ratio changes result in dramatic weight and power decreases in the range of 10 to 30, as can be seen in Figure 4.9 and Figure 4.10. Above 30 however there is little benefit to increasing the aspect ratio and some disadvantage as bending moments increase and make it difficult to maintain wing rigidity. Below values of about 20, decreasing aspect ratio results in significant weight increases. This is consistent with initial assumptions. Since wingspan is constant, decreasing aspect ratio results in increased wing area which results in increased drag which results in greater propulsion power required which ultimately results in a higher W_{TO}. Based on these results, the Helios aspect ratio appears to suit the CRFC UAV design and therefore an aspect ratio of 30.9 is also used for the CRFC UAV.

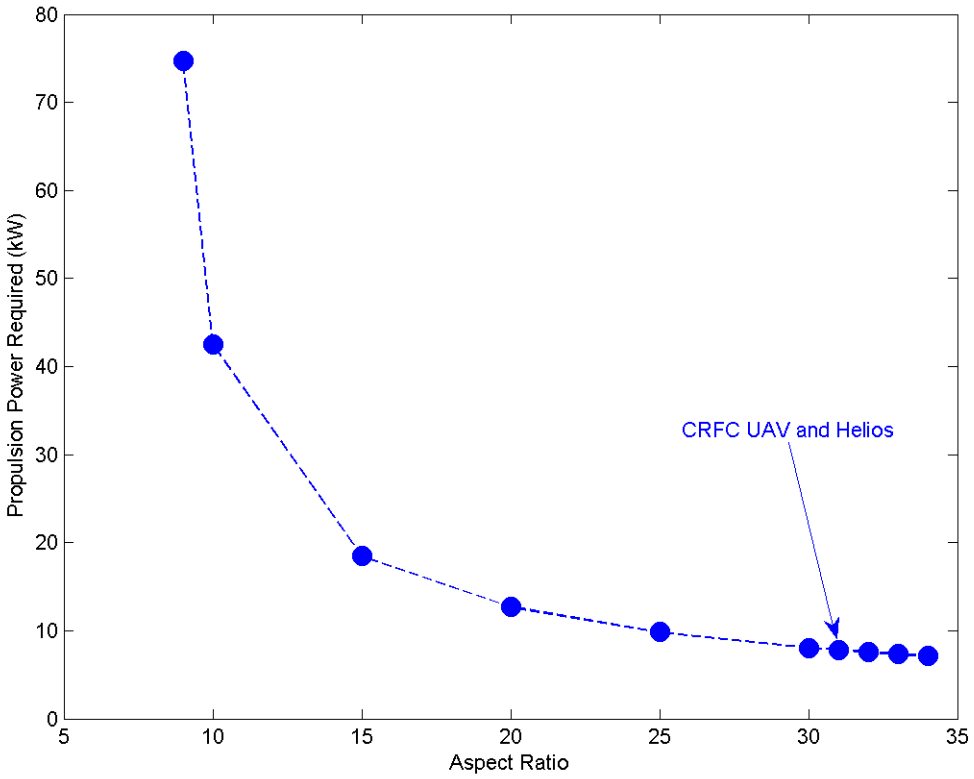

Figure 4.9: Relationship between power and aspect ratio

4.8 Wingspan

Wingspan is a key design parameter because it is what determines the sizing of the aircraft. The other wing dimensions as well as the empty weight scale with wingspan as shown in Equations (4.5), (4.6), (4.7), and (4.8).

$$chord = \frac{wingspan}{AR} \tag{4.5}$$

$$thickness = 0.12 \times chord \tag{4.6}$$

$$S = wingspan \times chord \tag{4.7}$$

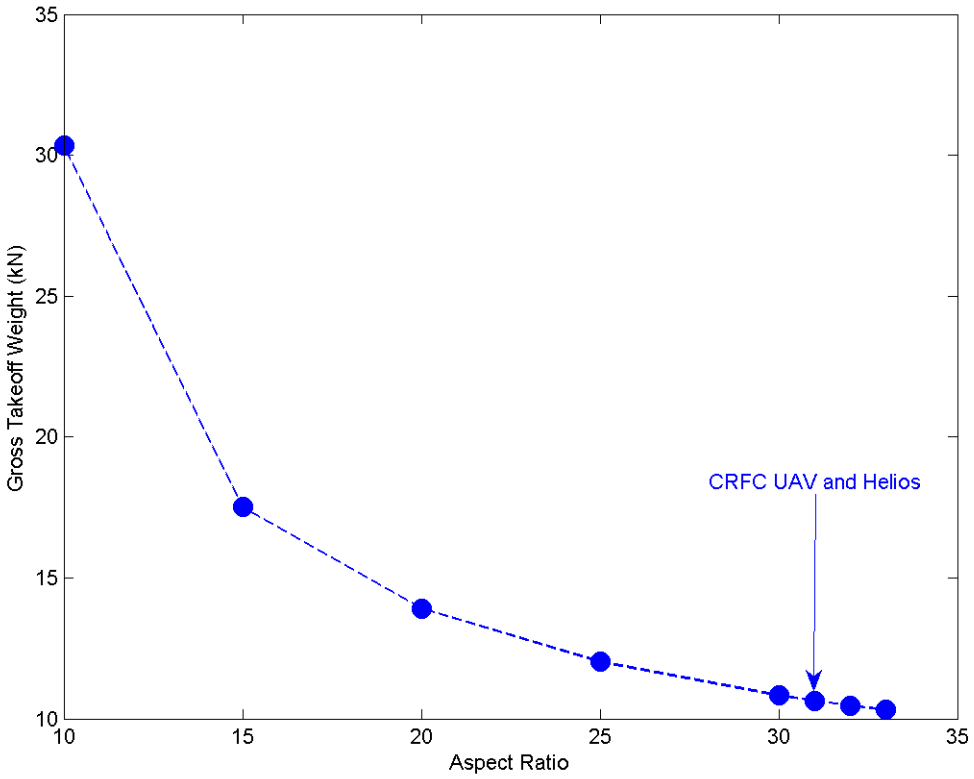

Figure 4.10: Relationship between gross takeoff weight and aspect ratio

$$W_E = \frac{2490}{75.29} \times wingspan \tag{4.8}$$

Note that a scaling factor is used to determine the W_E in Equation (4.8). The 2490 is the weight of the Helios prototype in N while the 75.29 is the Helios prototype wingspan in m. The weight/wingspan ratio multiplied by our chosen wingspan yields an estimate of W_E at that wingspan.

Figures 4.11 and 4.12 show how takeoff weight and peak glucose production rate vary with wingspan. The limiting condition for this parameter is a wingspan of less than 95 m. Below 95 m, the wing can not generate sufficient lift at the given cruise velocity. On the high end, we once again wish to avoid the bending moments of an overly large wing.

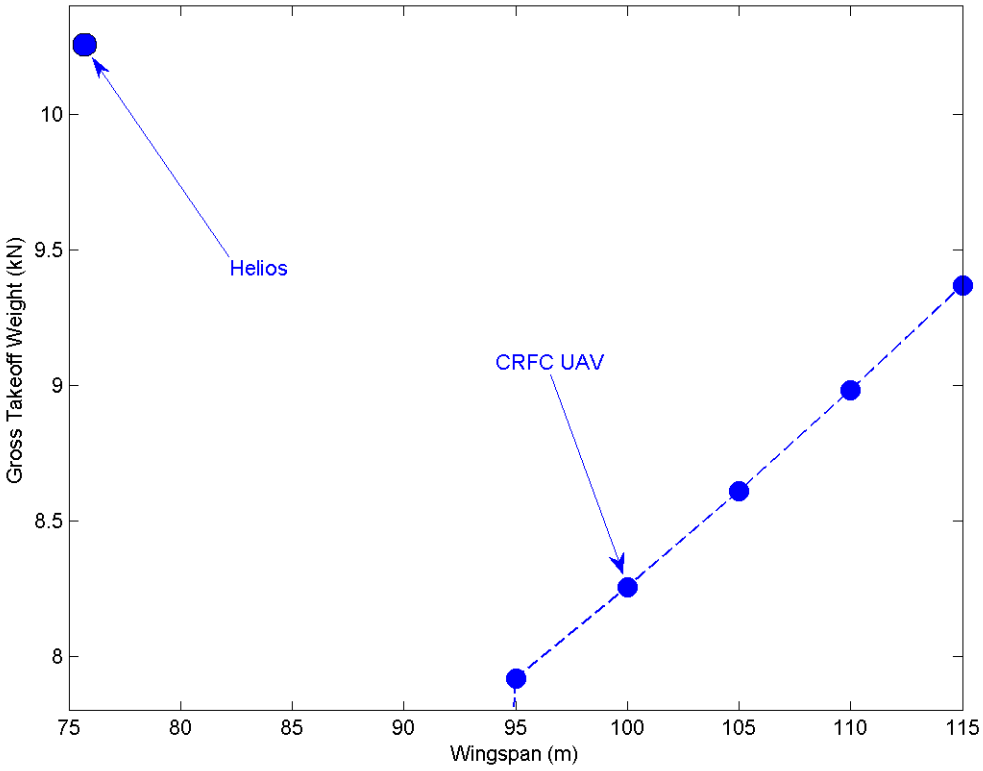

Figure 4.11: Relationship between gross takeoff weight and wingspan

4.9 Helios Comparison

In order to present as accurate a comparison with the Helios prototype as possible, certain CRFC UAV design values are changed from those chosen for an operational mission to comparison values which are chosen to mimic the design of the Helios prototype as closely as possible. The CRFC UAV parameters which have been altered specifically for the comparison in this section are presented in Table 4.1.

Table 4.1: Helios-representative Design Choices

Specification	Helios	Proposed CRFC UAV
Cruise Speed (m/s)	11.28 [*Noll et al.*, 2004]	20
Payload Weight (N)	0	1334.5
Wingspan (m)	75.29	100

The Helios-representative values from Table 4.1 are used to create a more accurately comparable CRFC UAV. This modified CRFC UAV is compared with the Helios

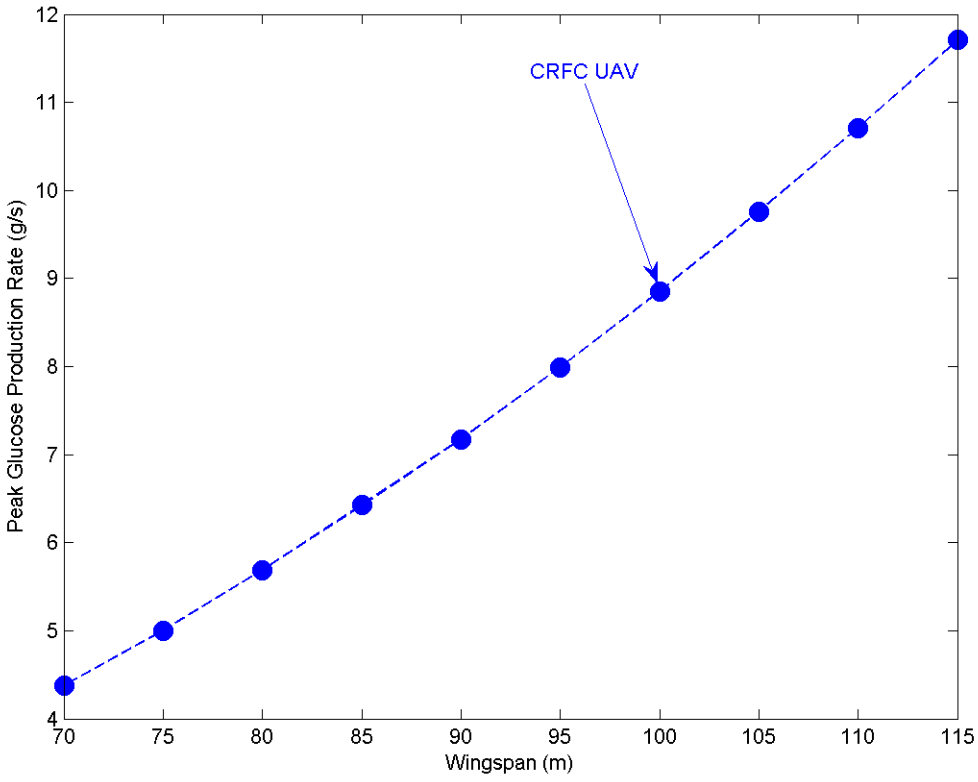

Figure 4.12: Relationship between peak glucose production rate and wingspan

prototype and the results are presented in Table 4.2. While every attempt is made to provide as meaningful a comparison as possible, it should be noted that the Helios vehicle in the stated configuration is only designed for a 7-14 day endurance [*Noll et al.*, 2004] while the proposed CRFC UAV is designed for NIE. The Helios power system weight is computed by adding the weight of the solar cells and batteries (see Section 3.5) to the additional weight of the consumable hydrogen fuel cell used on Helios' final flight [*Noll et al.*, 2004]. The planned regenerative hydrogen fuel cell was never flown due to time and budget constraints [*Noll et al.*, 2004]. The CRFC power system weight is computed by taking the sum of the fuel cell weight, the glucose reserve weight, and the algae layer weight. The difference between the fuel fraction of Helios and the proposed CRFC UAV is the key piece of data in Table 4.2. As shown in Table 2.1 and explained in Section 2.2, the 16 MJ/kg energy density of glucose is far more favorable for airborne applications

than the 0.68 MJ/kg energy density of batteries. The results in Table 4.2 clearly show the weight advantage of a CRFC as an airborne power source.

Table 4.2: Helios Comparisons

Specification	Helios	Proposed CRFC UAV	Percent Difference
Takeoff Weight (N)	10,320[*Noll et al.*, 2004]	3,725	64%
Power System Weight (N)	7,172	1,235	83%
Fuel Fraction	69%	33%	52%

V. Conclusions

The goal of this research is to determine the feasibility of, and identify the most important areas for more detailed follow-on work in, designing a production-ready CRFC power system for UAVs. Such a system conserves mass and uses zooxanthellae algae to capture solar energy and store it in the form of glucose (See Equation (2.1)). The glucose is consumed by a glucose fuel cell to meet the power demands of the UAV. The waste products from the fuel cell combustion are the required ingredients for further glucose production by the algae (See Figure 1.2). This system has significant weight advantages over storing energy in batteries (See Table 4.2), and it even has an advantage over hydrogen fuel cells because of the weight penalty associated with compressing hydrogen to a usable volumetric energy density (See Section 2.2). The 52% reduction in fuel fraction obtained by using a CRFC power source on a UAV similar to the Helios prototype holds considerable promise. Since Helios achieved great breakthroughs in HALE aviation, the possibilities for a similar aircraft with a CRFC power source could allow UAVs to easily perform missions [*Air University Center for Strategy and Technology*, 2007] which are currently considered only notional.

There are certain design and technology choices that have a much greater effect on the size of a CRFC aircraft than other choices. Based on the results in Chapter IV, these are the areas which should be studied in more detail. The greatest possible improvements in aircraft size are possible from improving the density of photosynthetic gathering organisms in the photosynthetic skin. The design is very sensitive to changes in the photosynthetic skin thickness because a certain thickness is required to obtain a rapid enough glucose regeneration but too great a thickness results in an excessively heavy aircraft. Currently there is only a very narrow usable range of thicknesses but improved efficiency in the glucose generation process could allow even thinner and lighter photosynthetic skins. The second most significant improvement would come from a true flight-weight glucose fuel cell. Figure 4.4 shows a steep improvement from the power to weight ratio of 2.94 W/N estimated from existing glucose fuel cell technology to about a value of 10 W/N. Such a power to weight ratio increase could decrease the weight of the aircraft by 2000 N (over 26 %) from the limits of the current estimate. Power to weight

ratios greater than 10 would not yield very significant weight savings and the effort of achieving increases over 10 would be better invested in optimizing other areas of the aircraft design.

There are a number of areas related to this research which could yield very valuable information. These areas are listed in the following section.

5.1 Recommendations for future research

1. Applications in space could benefit from a regenerative power system that is potentially not susceptible to degradation over time. Especially once colonies on the Moon or Mars are established, the gradual decay of traditional photovoltaic cells and batteries over time would be problematic because transporting a replacement system to those locations would require significant cost, effort and advance planning.
2. The CRFC UAV system could still be significantly optimized. No effort was made in this work to find the optimum value for all parameters. The trends were studied and individual parameters were chosen with reasonable values but a thorough optimization effort would almost certainly increase system performance.
3. A model needs to be created for the irradiance decrease in increasing thicknesses of the algae layer, a relationship which may be linear or non-linear. This will allow an algae depth to be chosen which will optimize energy production per unit area. The current estimate of no irradiance decrease with increasing depth will break down if a terrestrial application is attempted and weight does not limit the depth of the algae layer.
4. A thorough thermodynamic analysis should be conducted on the system over time in a variety of environments. Since the zooxanthellae are sensitive to temperature, it must be closely regulated. Factors such as insulating photosynthetic skin, waste heat from the fuel cell, and unused infrared radiation must be balanced with the convective heat loss from the surface of the UAV.

5. Another aspect of the zooxanthellae which is not understood well enough is how their life cycle would impact the operation of a CRFC UAV. Actions may need to be taken to regulate the zooxanthellae population and provide for reuse of cellular material of deceased organisms, perhaps with a small population of decomposing microbes.

6. Improvements in the method of generating glucose could be attempted. This may involve either a method of placing more zooxanthellae into the algae layer, increasing the efficiency with which zooxanthellae generate glucose, or a completely different approach to generating glucose that would provide advantages in power to weight ratio or other factors.

7. Improvements in the power density of glucose fuel cells are required. In other words, development of a flight-weight glucose fuel cell would immediate reduce the weight of the aircraft and allow it to be smaller for a given payload capacity.

8. Analysis of a High Altitude Airship powered by a CRFC has some potential. This was abandoned in the past due to the significant power requirements required to move an aircraft with such a large drag cross sectional area. However, advances in morphing structures and the large surface area available for algae could make this application feasible.

9. Analysis should be performed for other locations and times. This work is only a snapshot of one location and one time of year. Perhaps a future researcher could compare actual missions occurring over varying locations and times. For example a 3 month mission flying over various countries in the Middle East. This analysis could also examine aircraft drift due to intermittent winds above the average wind speed and discuss methods of mitigation.

10. Another application for NIE platforms is in a close-range low-altitude setting. Applications range from soldiers in a hostile city needing a timely and persistent tactical surveillance and communications relay to forest rangers searching for lost hikers. The requirements for such a platform are different than those for a high-altitude platform therefore this application was not considered here.

11. Construction of an operational CRFC would validate the concept and help to discover additional factors related to their usefulness in airborne applications. It is quite likely that other areas of research are still required to make a CRFC UAV a reality but these will not be discovered until a working model is actually constructed.

12. Research should also proceed in the use of CRFCs for terrestrial power generation. Given the recent emphasis on environmentally-friendly power production, this concept holds enormous promise. It is simple and safe enough that private residences could be equipped with this technology, paving the way to American energy independence.

The potential applications of CRFCs are truly staggering. Other than use on various airframes, CRFCs could be used in terrestrial power plants, in extraterrestrial power plants, as satellite power supplies, as power supplies for certain naval vessels, etc. The components could also be separated allowing glucose-powered vehicles and naturally glucose-producing fuel stations. If the technology became affordable enough, people could even have their own glucose-generating facility at their house to power their home and other devices, including the aforementioned vehicles.

Given the potential for significant improvement in this very new field, it is strongly suggested that more research be conducted on the two key improvements identified in Chapter V. With a relatively minimal investment, it would be possible to determine how practical the CRFC technology could be immediately and how long it might take for it to reach certain benchmarks of performance.

Appendix A. Matlab® Code

This is a representative copy of the Matlab® code used to perform the sizing analysis. This code is used to determine how the aircraft changes with changing aspect ratio as shown in Section 4.7.

A.1 Representative Sizing Code

Listing A.1: CRFC UAV sizing with varying AR

```
%% Glucose Powered UAV Code
% Capt Olek Wojnar
% Thesis Work for MS in Aeronautical Engineering
% Air Force Institute of Technology
% Class 08M

%% Notation format:
% constant/variable = value; % constant/variable definition (units, ...
    if required) (source or other relevant info)

close all; clear all; clc;

%% Global Constants

g = 9.81; % acceleration due to gravity (m/s^2)
EnergyDensity_Glucose = 16000000; % Energy Density of Glucose (J/kg)
LightEnergySun = 502.9; % Light power per unit area entering Earth's...
     atmosphere from the Sun in 400-700nm wavelength(W/m^2)
density_water = 997.04; % Density of water at 25 degrees C (kg/m^3)
SW_water = density_water*g; % Specific weight of water (N/m^3)
watts_to_einsteins = 550/119.6; % Conversion factor from W/m^2 to ...
    microE/(m^2s) at average wavelenght of 550nm (La Point pg 66)
photo_rate_slope = 0.45; % Slope of Phototsynthetic Rate vs Light ...
    Intensity curve (Fitt pg 23)
pgO2_to_kgGlucose = 180/((1e12)*32*3600*6*1000); % Conversion factor...
     from picograms of O_2 produced per hour per alga to kg of ...
    Glucose produced per second per alga (reference Section 2.1)

%% Start parameter characterization loop

% Parameter to characterize
c_x = [9 10 15 20 25 30 31 32 33 34]; % Parameter range
for characterize = 1:size(c_x,2);
     AR = c_x(characterize);

%% Mission parameters (move inside loop if changing over the course ...
    of the mission)
current_time = datenum('March 28, 2008 23:00:00.000'); % Zulu ...
    starting time (days) (~local sunset)
location.longitude = -84.1; % longitude of Dayton (degrees)
location.latitude = 39.8; % lattitude of Dayton (degrees)
location.altitude = 20000; % loiter altitude of aircraft (m)
```

```
Velocity = 20; % aircraft velocity (m/s)
rho = .0889; % air density (kg/m^3)
eta_prop = 0.92; % prop efficiency (Harmats pg 327)
eta_motor = 0.90; % motor efficiency (Harmats pg 328)
eta_FuelCell = 0.81; % fuel cell efficiency (Chaudhuri pg 1230)
eta_SkinCover = .99; % transmittance of algae cover (for ...
    photosynthetic wavelengths, borosilicate crown glass, CRC 70th Ed...
     pg E-422)
algal_density = 5.5681e14; % Density of algae in fluid medium (alga/...
    m^3) (Modified to allow enough exergy production 1/10 of ...
    theoretical max)
algae_layer_thickness = .0001; % Depth of fluid-filled cavity ...
    containing algae (m)
electrolyte_per_area_reference = 0.0105; % Volume of electrolyte ...
    with H2O density per unit area of electrode (m^3/m^2) (Chaudhuri ...
    pg 1229/1231)
electrolyte_per_area = electrolyte_per_area_reference/10000; % ...
    Scaling factor to reduce thickness of electrolyte layer. Since ...
    Chaudhuri says most of reaction occurs on electrode surface ...
    anyway.
PowerDensityFuelCell = .031; % Power density of fuel cell per area ...
    of electrode (W/m^2) (Chaudhuri pg 1230)
FuelCellElectrodeAreaDensity = 0.000027; % Fuel Cell Electrode Area ...
    Density (kg/m^2) (Zhang pg 1216)
FuelCellElectrolyteAreaDensity = density_water*electrolyte_per_area...
    ; % Fuel Cell Electrolyte Area Density (kg/m^2)
PowerWeightFuelCell = PowerDensityFuelCell/((...
    FuelCellElectrodeAreaDensity + FuelCellElectrolyteAreaDensity)*g)...
    ; % Power to Weight ratio of Fuel Cell (W/N)

GlucoseConcentration = 0.45; % Mass Concentration of Glucose to ...
    water, using just below max solubility at 25 degrees C to save ...
    weight(Mark Bishop URL)
EnergyDensity_Total = EnergyDensity_Glucose*GlucoseConcentration; % ...
    Total energy density of glucose fuel slurry (J/kg)
e = .9; % Oswald Efficiency Number (high since long and tapered)
% AR = 30.9; % Aspect Ratio (from NASA Helios)
wingspan = 100; % Wingspan (m) (adapted to allow reasonable C_L ...
    numbers)
wingchord = wingspan/AR; % Chord of wing (m)
wingthickness = .12*wingchord; % Thickness of wing (m) (from NASA ...
    Helios ratio)
S = wingspan*wingchord; % wing planform area (m^2)
PayloadWeight = 1334.5; % Payload Weight (N) (Hicks) (Helios Max...
    =329.308 kg)
AuxPowerRequired = 20; % Power required by auxiliary aircraft ...
    systems (W)
PayloadPowerRequired = 600; % Power Required by Payload (W) (Hicks)
iterate_fuel_cell_weight(1) = 150; % Initial iteration of fuel cell ...
    weight (N)
iterate_glucose_reserve(1) = 1500; % Initial iteration of glucose ...
    reserve weight (N)
algae_layer_weight(1) = algae_layer_thickness*S*SW_water; % Initial ...
    iteration of algae layer weight (N)
```

```
W_E(1) = 2490*wingspan/75.29; % Empty weight based on scaling ...
    factors (N) (from NASA helios)
W_TO(1) = W_E(1) + PayloadWeight + iterate_fuel_cell_weight(1) + ...
    iterate_glucose_reserve(1) + algae_layer_weight(1); % Calculated ...
    initial iteration of Gross Takeoff Weight (N)
AtmosphericLossFactor = 1; % High altitude, assume no atmospheric ...
    losses
LightEnergyAlgae = LightEnergySun*AtmosphericLossFactor*...
    eta_SkinCover; % Maximum light energy flux per unit area ...
    available to algae (W/m^2)

%% Sizing routine start
MaxIterations = 20; % Maximum number of iterations
ConvergenceFraction = .005; % Maximum percent difference between ...
    most recently calculated and previous wingspan to achieve ...
    convergence

 for iLoop = 1:MaxIterations
     exergy_weight_temp = 0; % Initialize temporary variable for ...
         glucose weight calculations (N)

%% Time control and initial values
time_step = 60; % length of each iteration (s)
run_time = 60*24; % number of time steps to run. (60*24=1 day, for...
     60 second timestep)

for t_ctr = 1:run_time
     current_time = current_time + time_step/(3600*24); % increment ...
         the time (days)

%% Light Calculations
     sun_time = datestr(current_time, 'dd-mmm-yyyy HH:MM:SS'); % ...
         convert to a format that the sun_position function will ...
         accept
     sun = sun_position(sun_time, location); % send time and location...
          to sun_position code
     incidence(t_ctr) = sun.zenith; % Sun angle from local vertical (...
         degrees)

     if cosd(incidence(t_ctr)) > 0
       useful_light(t_ctr) = cosd(incidence(t_ctr))*LightEnergyAlgae...
           ; % Light energy flux per unit area at given location/time...
            (W/m^2)
     else
         useful_light(t_ctr) = 0; % No light energy input if the sun ...
             is below local horizontal
     end

%% Drag Calucations
     % Drag computation neglects wave drag since at cruising speed M...
         <<1
     CL(characterize) = 2*W_TO(iLoop)/(S*rho*Velocity^2); % ...
         Coefficient of Lift
     CD_o = 0.03; % Coefficient of Parasitic Drag
```

```
        CD_L(characterize) = CL(characterize)^2/(pi*e*AR);% Coefficient ...
            of Induced Drag
        CD(characterize) = CD_o + CD_L(characterize); % Coefficient of ...
            Drag
100     D(t_ctr,characterize) = .5*rho*Velocity^2*S*CD(characterize); % ...
            Drag (N)

    %% Power Calculations
        PropulsionPowerRequired(t_ctr) = D(t_ctr,characterize)*Velocity...
            ; % Power required by propulsion system (W)
        TotalPowerRequired(t_ctr) = PropulsionPowerRequired(t_ctr)/...
            eta_prop/eta_motor + PayloadPowerRequired + AuxPowerRequired...
            ; % Total Power
105




        ExergyDestructionRate(t_ctr) = TotalPowerRequired(t_ctr)/...
            eta_FuelCell; % Rate of Exergy consumption (W)
        mdot_glucose_consumed(t_ctr) = ExergyDestructionRate(t_ctr)/...
            EnergyDensity_Total; % Rate of glucose slurry consumption (kg...
            /s)
        ExergyCreationRate(t_ctr) = useful_light(t_ctr)*S; % Max ...
            Theoretical rate of Exergy creation if 100% of light is ...
            converted (W)
        mdot_glucose_produced(t_ctr) = useful_light(t_ctr)*...
            watts_to_einsteins*photo_rate_slope*pgO2_to_kgGlucose*...
            algal_density*algae_layer_thickness*S/GlucoseConcentration; %...
             Rate of glucose slurry creation (kg/s) (reference Section...
             2.1)
110     mdot_glucose(t_ctr) = mdot_glucose_produced(t_ctr) - ...
            mdot_glucose_consumed(t_ctr); % Net glucose creation rate (kg...
            /s)
        if ExergyCreationRate(t_ctr) <= 0
             glucose_efficiency(t_ctr) = 0;
        else
             glucose_efficiency(t_ctr) = mdot_glucose_produced(t_ctr)/(...
                ExergyCreationRate(t_ctr)/EnergyDensity_Total); % ...
                Efficiency of glucose creation from light
115     end

    %% Weight Calculations
        exergy_weight(t_ctr) = exergy_weight_temp + mdot_glucose(t_ctr)*...
            time_step*g; % Total weight of glucose created (N)
        if exergy_weight(t_ctr) > 0 % We can't create more glucose than ...
            we have room for in our tanks
120          exergy_weight(t_ctr)= 0;
        end
        exergy_weight_temp = exergy_weight(t_ctr); % Temporary variable ...
            for glucose weight calculations (N)
```

```
        fuel_cell_weight(t_ctr) = TotalPowerRequired(t_ctr)/...
            PowerWeightFuelCell; % Minimum weight of required fuel cell (...
            N)

%% End Time Loop
end

%% Sizing routine end
            iterate_glucose_reserve(iLoop+1) = abs(min(exergy_weight))...
                ; % Minimum weight of glucose reserve (N) (assume tank ...
                weight is part of aircraft structure)
            algae_layer_weight(iLoop+1) = algae_layer_thickness*S*...
                SW_water; % Weight of algae layer, using weight of water...
                 (N)
            iterate_fuel_cell_weight(iLoop+1) = abs(max(...
                fuel_cell_weight)); % Weight of required fuel cell (N)
            W_E(iLoop+1) = 2490*wingspan/75.29; % Empty weight based on...
                 scaling factors (N) (from NASA helios)

            % So we don't overshoot
            iterate_glucose_reserve(iLoop+1) = iterate_glucose_reserve(...
                iLoop) + (iterate_glucose_reserve(iLoop+1) - ...
                iterate_glucose_reserve(iLoop))/1.5; % Incremement by ...
                fraction of difference
            algae_layer_weight(iLoop+1) = algae_layer_weight(iLoop) + (...
                algae_layer_weight(iLoop+1) - algae_layer_weight(iLoop))...
                /1.5; % Incremement by fraction of difference
            iterate_fuel_cell_weight(iLoop+1) = ...
                iterate_fuel_cell_weight(iLoop) + (...
                iterate_fuel_cell_weight(iLoop+1) - ...
                iterate_fuel_cell_weight(iLoop))/1.5; % Incremement by ...
                fraction of difference

            W_TO(iLoop+1) = W_E(iLoop+1) + PayloadWeight + ...
                iterate_fuel_cell_weight(iLoop+1) + ...
                iterate_glucose_reserve(iLoop+1) + algae_layer_weight(...
                iLoop+1); % Actual Aircraft Takeoff Weight (N)

             if abs(W_TO(iLoop+1)-W_TO(iLoop))/W_TO(iLoop+1) <= ...
                 ConvergenceFraction
                 if exergy_weight(end)-exergy_weight(1) < 0
                     c_W_TO(characterize) = 0;
                 fprintf('NIE unachievable!!\n');
                 else
                     c_W_TO(characterize) = W_TO(iLoop+1);
                 end

                 if CL(characterize) > 1.6
                     c_W_TO(characterize) = 0;
                 fprintf('CL unachievable!!\n');
                 end
                 break
             end

             if iLoop == MaxIterations
```

```
                    fprintf('Weight NOT converged!!\n');
                    c_W_TO(characterize) = 0;
                end
160             c_P(characterize) = max(PropulsionPowerRequired);

        end %sizing iteration

    %% End parameter characterization loop
165 disp(sprintf('%g\n',size(c_x,2)-characterize));
    end

    %% Show Results

170 figure1 = figure;
    axes('Parent',figure1);
    box('on');
    hold('all');

175
    % plot(c_x,c_W_TO,'MarkerFaceColor',[0 0 1],'MarkerSize',10,'Marker...
       ','o','LineWidth',1,'LineStyle','--');
    % xlabel('Aspect Ratio');
    % ylabel('Gross Weight (N)');
    % annotation(figure1,'textarrow',[0.7821 0.7804],[0.3699 0.1429],...
180 %     'TextEdgeColor','none',...
    %     'String',{'CRFC UAV and Helios'},...
    %     'Color',[0 0 1]);
    % filename = strcat('I:\My Documents\Thesis\WojnarThesis\Chapter4\...
       figures\UAV_AR_weight');

185 plot(c_x,c_P,'MarkerFaceColor',[0 0 1],'MarkerSize',10,'Marker','o',...
       'LineWidth',1,'LineStyle','--');
    xlabel('Aspect Ratio');
    ylabel('Propulsion Power Required (W)');
    annotation(figure1,'textarrow',[0.7589 0.8],[0.4294 0.2024],...
        'TextEdgeColor','none',...
190     'String',{'CRFC UAV and Helios'},...
        'Color',[0 0 1]);
    filename = strcat('I:\My Documents\Thesis\WojnarThesis\Chapter4\...
       figures\UAV_AR_power');

    print('-dpng',filename)
```

Bibliography

Air University Center for Strategy and Technology (2007), Blue Horizons 2007 "Horizon 21" Project Report, *Tech. rep.*, Air University Center for Strategy and Technology.

Bishop, M. (2005), An introduction to chemistry.

Buchmann, I. (2006), Battery University.

Chaudhuri, S. K., and D. R. Lovley (2003), Electricity generation by direct oxidation of glucose in mediatorless microbial fuel cells, *Nature biotechnology*, *21*(10), 1229–1232.

Curry, M. (2007), NASA Dryden Fact Sheet - Helios Prototype.

Curry, M. (2008), NASA Dryden Fact Sheet - Solar-Power Research and Dryden.

Dereniak, E. L., and D. G. Crowe (1984), *Optical radiation detectors*, 300 pp., John Wiley and Sons, Inc., New York, NY.

Ehrenman, G. (2004), From foul to fuel, *Mechanical Engineering*, *126*(6), 32–33.

Finneran, K. T., C. V. Johnsen, and D. R. Lovley (2003), Rhodoferax ferrireducens sp. nov., a psychrotolerant, facultatively anaerobic bacterium that oxidizes acetate with the reduction of Fe(III), *Int J Syst Evol Microbiol*, *53*(3), 669–673.

Fitt, W. K., and C. B. Cook (2001), Photoacclimation and the effect of the symbiotic environment on the photosynthetic response of symbiotic dinoflagellates in the tropical marine hydroid myrionema amboinense, *J.Exp.Mar.Bio Ecol.*, *256*(1), 15–31.

Food and Agriculture Organization of the United Nations (2003), Food energy methods of analysis and conversion factors, Report of a technical workshop - Rome, 36 December 2002, *Tech. rep.*, Publishing Management Service, Information Division, FAO.

Freedom Car and Fuel Partnership (2005), Hydrogen storage technologies roadmap, *Tech. rep.*

Garcia, R. L., S. B. Idso, and B. A. Kimball (1994), Net Photosynthesis as a Function of Carbon-Dioxide Concentration in Pine Trees Grown at Ambient and Elevated CO2, *Environmental and experimental botany*, *34*(3), 337–341.

Gray, F. (1991), Trends in U.S. production and use of glucose syrup and dextrose, 1965-1990, and prospects for the future, *Tech. rep.*, U.S. Department of Agriculture, Economic Research Service.

Harmats, M., and D. Weihs (1999), Hybrid-propulsion high-altitude long-endurance remotely piloted vehicle, *Journal of Aircraft*, *36*(2), 321.

Hicks, K. (2002), Global Hawk Program Update, *Tech. Rep. ASC 02-1348*, USAF.

La Point, T. W., F. T. Price, E. E. Little, and ASTM Committee E-47 on Biological Effects and Environmental Fate. and Environmental Toxicology and Risk Assessment (1996), Environmental toxicology and risk assessment, fourth volume, ASTM, West Conshohocken, PA.

Merriam-Webster Online (2007), Definition of "fuel cell".

National Oceanic and Atmospheric Administration (2008), Monthly/seasonal climate composites.

Noll, T. E., J. M. Brown, M. E. Perez-Davis, S. D. Ishmael, G. C. Tiffany, and M. Gaier (2004), Investigation of the Helios Prototype Aircraft Mishap, Volume I Mishap Report, *Tech. rep.*

Reda, I., and A. Andreas (2004), Solar position algorithm for solar radiation applications, *Solar Energy*, *76*(5), 577.

Rhodes, J. P. (1993), Chronology: The Army Air Corps to World War II.

Shulski, M. D., E. A. Walter-Shea, K. G. Hubbard, G. Y. Yuen, and G. Horst (2004), Penetration of photosynthetically active and ultraviolet radiation into alfalfa and tall fescue canopies, *Agronomy Journal*, *96*(6), 1562–1571.

Turns, S. R. (2000), *An Introduction to Combustion: Concepts and Applications*, 676 pp., McGraw-Hill.

United States Department of Energy (2007), Types of fuel cells.

Velev, O. A. (2000), Regenerative fuel cell system for an unmanned solar powered aircraft, *AIAA Paper 2000-2873*.

Von Stetten, F., S. Kerzenmacher, A. Lorenz, V. Chokkalingam, N. Miyakawa, R. Zengerle, and J. Ducree (2006), A one-compartment, direct glucose fuel cell for powering long-term medical implants, in *19th IEEE International Conference on Micro Electro Mechanical Systems*, vol. 2006, pp. 934–937.

Weibel, M. K., and C. Dodge (1975), Biochemical fuel cells , : Demonstration of an obligatory pathway involving an external circuit for the enzymatically catalyzed aerobic oxidation of glucose, *Archives of Biochemistry and Biophysics,*, *169*(1), 146–151.

Zhang, B., J. Liang, C. L. Xu, B. Q. Wei, D. B. Ruan, and D. H. Wu (2001), Electric double-layer capacitors using carbon nanotube electrodes and organic electrolyte, *Materials Letters,*, *51*(6), 539–542.

Zhang, M., S. Fang, A. A. Zakhidov, S. B. Lee, A. E. Aliev, C. D. Williams, K. R. Atkinson, and R. H. Baughman (2005), Strong, transparent multifunctional, carbon nanotube sheets, *Science*, *309*(5738; 5738), 1215–1219.

REPORT DOCUMENTATION PAGE

Form Approved
OMB No. 0704–0188

1. REPORT DATE (DD–MM–YYYY)	2. REPORT TYPE	3. DATES COVERED *(From — To)*
27–03–2008	Master's Thesis	Mar 2007 — Mar 2008

4. TITLE AND SUBTITLE

Analyzing Carbohydrate-Based Regenerative Fuel Cells as a Power Source for Unmanned Aerial Vehicles

5a. CONTRACT NUMBER

5b. GRANT NUMBER

5c. PROGRAM ELEMENT NUMBER

6. AUTHOR(S)

Olek Wojnar, Capt, USAF

5d. PROJECT NUMBER

5e. TASK NUMBER

5f. WORK UNIT NUMBER

7. PERFORMING ORGANIZATION NAME(S) AND ADDRESS(ES)

Air Force Institute of Technology
Graduate School of Engineering and Management (AFIT/EN)
2950 Hobson Way
WPAFB OH 45433-7765

8. PERFORMING ORGANIZATION REPORT NUMBER

AFIT/GAE/ENY/08-M31

9. SPONSORING / MONITORING AGENCY NAME(S) AND ADDRESS(ES)

N/A

10. SPONSOR/MONITOR'S ACRONYM(S)

11. SPONSOR/MONITOR'S REPORT NUMBER(S)

12. DISTRIBUTION / AVAILABILITY STATEMENT

APPROVED FOR PUBLIC RELEASE; DISTRIBUTION UNLIMITED

13. SUPPLEMENTARY NOTES

14. ABSTRACT

Based on current capabilities, we examine the feasibility of creating a carbohydrate-based regenerative fuel cell (CRFC) as the primary power source for unmanned aerial vehicles (UAV) for long endurance missions where station keeping is required. A CRFC power system is based on a closed-loop construct where carbohydrates are generated from zooxanthellae, algae that create excess carbohydrates during photosynthesis. The carbohydrates are then fed to a carbohydrate fuel cell where electric power is generated for the UAV's propulsion, flight control, payload, and accessory systems. The waste products from the fuel cell are used by the zooxanthellae to create more carbohydrates, therefore mass is conserved in the process of power generation. The overall goal of this research is to determine if CRFCs should be explored further as a viable power source. Through simulations, a UAV is sized to determine if greater than 24 hour endurance flight is possible and these results are compared to UAVs using more traditional photocell based power systems. The initial results suggest that more research should be done in the development of CRFCs as a power system for long endurance UAVs. The final outcome of this research is to identify the most important areas for more detailed follow-on work in designing a production-ready CRFC power system for long endurance UAVs.

15. SUBJECT TERMS

Fuel cells, glucose, unmanned, aircraft design, aircraft power sources, all wing aircraft, observation aircraft, reconnaissance aircraft, high altitude, long endurance.

16. SECURITY CLASSIFICATION OF:			17. LIMITATION OF ABSTRACT	18. NUMBER OF PAGES	19a. NAME OF RESPONSIBLE PERSON
					Maj Eric D. Swenson
a. REPORT	b. ABSTRACT	c. THIS PAGE	UU	62	19b. TELEPHONE NUMBER (Include Area Code) (937) 255-3636, ext 7479; e-mail: Eric.Swenson@afit.edu
U	U	U			